629.1309
U354
Y 3.N21/5:16/2468
GOVT. DOC.
NACA TN 2468

NATIONAL ADVISORY COMMITTEE FOR AERONAUTICS

TECHNICAL NOTE 2468

INVESTIGATION AT LOW SPEED OF 45° AND 60° SWEPTBACK, TAPERED, LOW-DRAG WINGS EQUIPPED WITH VARIOUS TYPES OF FULL-SPAN, TRAILING-EDGE FLAPS

By John J. Harper

Georgia Institute of Technology

Washington

October 1951

CONN. STATE LIBRARY
BUSINESS, SCIENCE & TECHNOLOGY DEP'T.
OCT 17 1951

NATIONAL ADVISORY COMMITTEE FOR AERONAUTICS

TECHNICAL NOTE 2468

INVESTIGATION AT LOW SPEED OF 45° AND 60° SWEPTBACK, TAPERED, LOW-DRAG WINGS EQUIPPED WITH VARIOUS TYPES OF FULL-SPAN, TRAILING-EDGE FLAPS

By John J. Harper

SUMMARY

An investigation was made in the Georgia Institute of Technology 9-foot wind tunnel to determine the low-speed aerodynamic characteristics of two sweptback, low-drag, tapered wings equipped with full-span split and slotted flaps and three special types of trailing-edge flaps. Two sweep angles of 45° and 60°, measured at the quarter chord, were used.

Although emphasis was placed on attempts to obtain higher maximum lift coefficients, the results show no appreciable gain in $C_{L_{max}}$ for either the split flap or the special flaps on the 60° wing. These same flaps did produce an increment in $C_{L_{max}}$ on the 45° model, however. The slotted flap produced by far the largest increase in lift on both models.

The effect of the flaps on drag and pitching moment is the same as that indicated by other test data available. The slotted flap caused the largest increase in pitching moment for a given deflection angle. All flap configurations increased the stability of both wings.

INTRODUCTION

The use of large amounts of sweep for the purpose of delaying compressibility effects is now quite common and was originally proposed in this country by Jones (reference 1). Unfortunately, the use of wing plan forms incorporating large sweep angles in conjunction with the thin airfoil sections necessary for high critical Mach numbers has resulted in wings having values of maximum lift considerably less than those of conventional straight wings. This has imposed rather severe limitations upon the landing speeds of such aircraft.

Although the usual trailing-edge type of high-lift devices may be employed on swept wings, German data (reference 2) have indicated that the conventional split and slotted flaps do not show the same gains in maximum lift coefficient on sweptback wings.

A considerable amount of German test data (references 2 and 3) on flapped sweptback wings is available, but seemingly little work has been done toward increasing the maximum lift coefficient by eliminating or reducing the sweep angle of the flap itself. In order to determine whether such flaps were feasible, a test program of an exploratory nature was instigated. The present tests have also supplemented the results of references 4 and 5.

This work was conducted at the Georgia Institute of Technology under the sponsorship and with the financial assistance of the National Advisory Committee for Aeronautics.

APPARATUS AND MODELS

Two semispan sweptback wing models were tested in the 9-foot wind tunnel of the Georgia Institute of Technology. This tunnel is of the single-return type having a closed circular test section 12 feet long. For panel testing a flat floor is installed which gives a jet height of approximately 8 feet. Speed changes are accomplished by means of a controllable-pitch propeller. The tunnel turbulence factor is 1.7.

Two models of 45° and 60° sweep were mounted on a 50-inch-diameter plywood disk as shown in figure 1. This disk had approximately 1/4-inch clearance all around. The two wings were constructed to the plan forms shown in figures 2 and 3. The airfoil, maintained parallel to the plane of symmetry, was of NACA 65A006 profile, the ordinates for which are given in table I. Because of the extremely thin airfoil used and the small taper ratio (0.6), it was impossible to construct the models of laminated mahogany in the usual manner. A built-up rib-spar construction was employed with the models being covered with 1/8-inch aluminum-alloy sheet, except for the portion ahead of the front spar where laminated mahogany was used.

With the exception of the slotted flap, all flaps were constructed of 1/8-inch aluminum-alloy sheet attached to the wing by means of piano hinges. The slotted flap was constructed of laminated mahogany to the NACA 4412 profile. The hinge point was somewhat arbitrarily located at x = 100 percent c, and y = -2.5 percent c, since the data of reference 6 indicate that this is the optimum location on a straight wing. The slotted flap was attached to the model by means of steel

brackets. All flaps had a system of links that enabled settings of 15°, 30°, 45°, and 60° to be made. Figures 4 and 5 are photographs of the various flaps tested on the two wings. The various flap arrangements on both models are shown schematically in figures 6 and 7. The special flaps were obtained by cutting off and rotating the original flap to reduce the sweep angle of the hinge axis.

All flaps were full-span and were 30 percent of the chord measured parallel to the plane of symmetry. This resulted in a flap area of approximately 2.26 square feet for the split and slotted flap on both models. This gave a ratio of flap area to wing area S_f/S of 0.28. The special flaps had a very slightly smaller area because of cutting of the conventional flaps. See figures 2 and 3 for dimensions.

Because of excessive vibration and deflection of the 60° wing, it was necessary to use a brace wire as shown in figure 5.

SYMBOLS

All moments are referred to the quarter-chord point of the mean aerodynamic chord.

A	aspect ratio $(b^2/2S)$
b	twice span of semispan model, feet
C_D	drag coefficient (D/qS)
ΔC_D	increment of drag coefficient due to flap deflection
C_L	lift coefficient (L/qS)
$C_{L_{max}}$	maximum lift coefficient
ΔC_L	increment of lift coefficient
$\Delta C_{L_{max}}$	increment of maximum lift coefficient
Δc_l	increment of section lift coefficient

$C_{m_{c/4}}$ pitching-moment coefficient about quarter chord $(M/qS\bar{c})$

c local chord, measured in free-stream plane, feet

$\bar{c}$ mean aerodynamic chord, feet $\left(\dfrac{\int_0^{b/2} c^2 db}{\int_0^{b/2} c\ db}\right)$

D drag, pounds

L lift, pounds

M pitching moment, foot-pounds

q dynamic pressure, pounds per square foot $(\rho V^2/2)$

R Reynolds number $(\rho V\bar{c}/\mu)$

S area of semispan wing, square feet

V free-stream velocity, feet per second

α model angle of attack, degrees

δ deflection angle of high-lift device, measured in plane normal to hinge axis, degrees

Λ sweepback angle of quarter-chord axis, degrees

λ taper ratio $\left(\dfrac{\text{Tip chord}}{\text{Root chord}}\right)$

μ coefficient of viscosity

ρ mass density of air, slugs per cubic foot

C_{L_α} lift-curve slope $\left(dC_L/d\alpha\right)$

Subscripts:

e effective

f flap

CORRECTIONS TO DATA

Since no data were available for the boundary corrections of sweptback panel models (with reflection plane), corrections similar to those for unswept reflection-plane models were applied to the drag coefficient and angle of attack. The corrections applied are those given in reference 7. They are

$$\Delta C_{D_i} = \delta \frac{S}{C} C_L^2 = 0.0130 C_L^2$$

$$\Delta\alpha = 57.3 \frac{S}{C} C_L = 0.742 C_L$$

where

ΔC_{D_i} induced-drag increment

$\Delta\alpha$ increment of angle of attack

δ boundary correction factor (0.0516)

S wing area including reflection (16 sq ft)

C tunnel cross-sectional area (63.7 sq ft)

The data have also been corrected for the effect of the end plate and brace wire (used on 60° model only); blocking corrections as given in reference 8 have also been applied.

The data obtained at angles of attack greater than 30° may be less accurate, since, at high angles of attack, the tip of the wing was close to the tunnel wall and no additional corrections were applied for this condition. In view of this fact it is believed that the tunnel walls affect the values of $\Delta C_{L_{max}}$ less than those of $C_{L_{max}}$; therefore the increments of $C_{L_{max}}$ due to flap deflection are considered more quantitatively correct than the absolute values of the maximum lift coefficient.

No corrections were applied to the pitching-moment data.

TESTS

Because of limitations of test equipment, most of the tests on the 60° model were run at a dynamic pressure of 25.6 pounds per square foot, which corresponds to an indicated airspeed of 100 miles per hour, giving an effective Reynolds number of about 2,900,000 based on the mean aerodynamic chord of the wing. Split-flap runs were made at an indicated speed of 120 miles per hour giving R_e = 3,480,000. All tests on the 45° wing were run at an indicated airspeed of 120 miles per hour giving R_e = 3,480,000 for all flap configurations. An open-jet test was made on the 60° wing in order to compare the results with those of the closed jet. The open-jet data only indicated that the additive wall corrections were qualitatively correct since their use gave lift and drag curves falling between those for the open- and closed-jet data.

The force tests were run through an angle-of-attack range of -12° to stall in increments of 3°, except near the stall where the increment was in some instances reduced to 1°. The smaller increment was used so that the lift curve could be more accurately faired at the stall.

Tuft studies of the upper surface were made for both the models at low, medium, and high angles of attack.

RESULTS AND DISCUSSION

The results of the force tests are presented in figures 8 to 17; the increments of maximum lift coefficients against flap angle are shown in figures 18 and 19; the drag increment ΔC_D for the various flaps is presented in figures 20 and 21; tuft-study data are shown schematically in figure 22; and the variation of aerodynamic-center position with C_L is given in figure 23.

An effort was made to evaluate within the limitations of the test equipment the effect of Reynolds number. The results of these tests are presented in figure 24 and show no systematic variations over the range of test velocities.

The figures presenting the results of the tests are given in table II along with a list of the cross-plotted results.

Plain wings.- In general, the aerodynamic characteristics of the plain wings are similar to those previously reported in references 3, 4,

and 5. Although the maximum lift coefficient was very nearly the same for both wings, it was slightly less than that obtained for the same wing configurations in unpublished data from the Langley Aeronautical Laboratory of the NACA. According to these data the maximum lift coefficients obtained at $R = 3 \times 10^6$ were about 1.04 and 1.08 for the 45° and 60° wings, respectively. These values compare with 1.03 and 1.0 for the 45° and 60° wings reported herein. The decrease in $C_{L_{max}}$ for the 60° wing is apparently caused by the proximity of the tunnel wall at the stall. The measured stall angles of the 45° and 60° wings were approximately 27° and 41°, respectively. For the same wings, stall angles of 25° and 36° were obtained according to the above data.

The measured slopes of the lift curves were 0.0562 and 0.040 for the 45° and 60° wings, respectively. The values of lift-curve slopes obtained from tests made in the Langley two-dimensional low-turbulence pressure tunnel are 0.056 and 0.039 for the two wings. Theoretical values of 0.054 and 0.041, obtained by the method of reference 9, are in good agreement with the measured data. Because the curves of lift coefficient against angle of attack are decidedly nonlinear, the slopes were measured at $\alpha = 0°$.

Plots of C_L against α and C_L against $C_{m_{c/4}}$ for the plain wings are presented in figures 8 and 13. It is noted in figures 8 and 13 that the pitching-moment coefficients for zero flap deflection are not zero at zero lift as they should be for a symmetrical airfoil. This is believed to be caused primarily by tunnel flow angularity in combination with slight model inaccuracies. Although a flow-angularity survey in the vicinity of the wing tips was not made, calculations indicate that as little as $\frac{1}{4}°$ of flow misalinement at the wing tip could cause the pitching-moment curve to shift. A very small lift force acting at the extreme tip can cause a relatively large change in pitching moment because of the large moment arm existing between the 25 percent mean aerodynamic chord and the 25-percent-chord point of a portion of the extreme tip. The small lift force would hardly affect the angle of zero lift and, hence, is not noticeable on the lift curves.

In order to give a somewhat clearer picture of what might be expected in the way of performance, the glide angles of the two wings at $C_{L_{max}}$ were calculated and are listed in table III. While only qualitative, these values do give some indication of the sinking speed at $C_{L_{max}}$. The increase of glide angle with increasing sweep is in qualitative agreement with similar results given in reference 10.

The changes that occur in the lift and pitching-moment curves are related to the changes in wing tip loading. Both wings exhibited a rapid decrease in stability at moderate lift coefficients, apparently caused by the expected tip stall which shifts the center of pressure forward. This sudden change in slope of the pitching-moment curve occurred at about $C_L = 0.70$ and 0.5, for the 45° and 60° wings, respectively. This same trend is reported in reference 9. A slight increase in stability is noted for both wings at small angles of attack. Similar results have been previously discussed in reference 5.

The large aerodynamic-center shifts with lift coefficient are similarly associated with changes in tip loading. The unstable movement of the aerodynamic center was predicted, however, from the data of reference 10, which indicate that certain combinations of sweepback and aspect ratio will be unstable. A plot of aerodynamic-center shift is presented in figure 23 for both wings.

Tuft studies of the upper surface of the plain wings are shown schematically in figure 22. Additional studies using a single tuft on a probe revealed that the strong spanwise flow is detectable at 4 or 5 inches above the surface. This spanwise flow is particularly noticeable on the 60° wing in the range of $\alpha \approx 10°$ to 15°.

In general, the effects of the flaps were the same as those on straight wings, except for the decreased effectiveness. The flaps in some instances gave lower drag coefficients and smaller glide angles at maximum lift coefficient than were obtained for the straight wings. This effect is noted also in reference 10.

Split flaps.– The full-span split flap had a 30 percent chord and deflected normal to the 70-percent-chord line. The effectiveness of the flap was markedly reduced as it produced a maximum increment of lift coefficient of 0.18 at $\delta_f = 30°$ on the 45° panel and 0.055 at $\delta_f = 30°$ on the 60° model. The very small contribution of the flap on the 60° wing is in agreement with data given in references 2, 3, 5, and 9. As shown in figures 8 and 13, the angle of attack at stall was not appreciably reduced on either wing. Although the data are not presented, it should be mentioned that sealing the flap at the inboard end to prevent the air from flowing behind the flap increased its effectiveness at low angles of attack but had little effect on $C_{L_{max}}$. The increments of $C_{L_{max}}$ for various flap deflections are shown in figures 18 and 19.

The predicted values of ΔC_L were based on two-dimensional data and simple sweep theory. For a given split-flap deflection

$$\Delta C_L = \Delta c_l \cos^2 \Lambda$$

The only two-dimensional data available were those given in reference 11 for the NACA 65-006 airfoil section with a 60° split flap. The predicted and measured increments of lift coefficient are presented in figure 25. These data were extrapolated to zero sweep by fairing the curve through the experimental points to the values of ΔC_L and $\Delta C_{L_{max}}$ obtained from section data.

Another method (unpublished) for estimating ΔC_L at zero angle of attack from two-dimensional data utilizes a method for unswept wings outlined in reference 12. The equation, as modified to account for sweep, is $\Delta C_L = J \Delta c_l C_{L_{\alpha_\Lambda}} \cos \Lambda$, where J is a factor depending on aspect ratio, taper ratio, and flap span (reference 12) and $C_{L_{\alpha_\Lambda}}$ is the calculated lift-curve slope of the swept wing. It appears that theory overestimates the contribution of the full-span flap on a swept-back wing; however, for inboard split-flap spans up to 0.5b/2 the method described above will give, with reasonable accuracy, the lift contribution of the split flap at zero angle of attack. This method fails to give accurate estimates of ΔC_L for flap spans greater than 0.5b/2 because the outboard portion of the flap apparently suffers an abnormal loss in effectiveness on a sweptback wing. As shown in figure 25 the increments of lift at zero angle of attack are larger than those at maximum lift. The order of magnitude of this effect is about the same as that noted for straight wings.

The data in table III, while only qualitative, do indicate, as previously reported in reference 10, that the split flap actually reduces the glide angle at $C_{L_{max}}$ for the 45° wing, whereas the glide angle is increased on the 60° wing.

Deflection of the split flap increased the negative values of $C_{m_{c/4}}$ without appreciably changing the shape of the pitching-moment curve, except for a slight negative increase. The increase in stability was greater, however, for the 60° wing. The lift coefficient at which instability occurred was increased on both wings, thus reducing the aerodynamic-center shift on both wings.

For comparison, the aerodynamic-center shift, flaps down, is plotted in figure 23. This figure shows the somewhat greater range of stability obtainable with flaps down.

The variation of drag increment ΔC_D with flap deflection is presented in figures 20 and 21.

Three-step flap.- Since the flap effectiveness was thought to be reduced primarily because of the sweep of the hinge line, special flaps incorporated were designed to remove all or part of this sweep. The practicability of these devices may be questionable, but this investigation was concerned primarily with their aerodynamic qualities and not their structural adaptability. The full-span, three-step flap, arranged to deflect in three segments about an axis normal to the plane of symmetry for the 45° wing and an axis of 41°45' for the 60° wing (figs. 6 and 7), proved to be of little value. As shown in figures 9 and 18, a very slight gain in $C_{L_{max}}$ was realized on the 45° wing for deflections less than 45°. Figures 14 and 19 reveal that a decrement of lift resulted on the 60° wing for flap deflections greater than 15°. Possibly the turbulence created by the staggered arrangement may be partially responsible for the poor performance. These results confirm the data of low Reynolds number tests of a similar configuration reported in reference 2, which showed this type of flap on a 45° sweptback wing to be ineffective.

The increments of maximum lift coefficient for various deflections as shown in figures 18 and 19 indicate a negligible increase in $C_{L_{max}}$ on the 45° wing and a decrement of lift on the 60° wing. Table III shows that the three-step arrangement was about as effective as the plain split flap at $\alpha = 0°$. It is also noted that this flap had about the same effect on the glide angle, decreasing it on the 45° wing and increasing it on the 60° wing.

The effect on the pitching moment was similar to that of the split flap in that a slight increase in stability was noted. The increase in moment coefficient $C_{m_{c/4}}$ was not so great as that due to the split flap.

The increment of drag coefficient due to the flap is shown in figures 21 and 22.

Six-step flap.- The six-step flap arrangement shown in figures 6 and 7 was inferior to the split flap. Figures 19 and 20 show that $\Delta C_{L_{max}}$ was about half as large as for the plain split flap on the 45° wing,

whereas a large decrement of lift resulted on the 60° wing for deflections above 15°. The six-step arrangement was more effective than the three-step flap on the 45° wing. As indicated in table III, this flap produced more lift at $\alpha = 0°$ on the 45° wing than any of the others, with the exception of the two slotted flaps. At $\alpha = 0°$ it proved superior to the slotted flap on the 60° model. Its high-angle-of-attack performance is decidedly poor, however. It appears that, aside from structural difficulties, this flap would not be at all practical.

The flap effect on pitching moment was much the same as that of the split and three-step flaps. Again, compared with the split flap, the increase in diving moment was not so large on the 45° wing and a little greater on the 60° wing (figs. 10 and 15).

It is noted that, according to theory, the removal or reduction of the sweep of the hinge line of split-type flaps should increase the effectiveness of such flaps. It would appear that the test results are in direct contradiction with theory since both the three- and six-step flaps were less effective than the conventional split flap. This decreased effectiveness seems to be attributable to the combined effects of turbulent flow created by the staggered segments and the poorly located hinge lines. In particular, the six-step arrangement appeared to create considerable turbulence. This turbulence is believed to be the primary cause of the reduced effectiveness of this configuration since the six segments were properly located along the 70-percent-chord axis. In the case of the three-step arrangement both turbulence and flap location appear to be responsible for the ineffectiveness of this configuration. The outboard edge of each of the three segments was located, as may be seen in figures 4 to 7, quite far forward on the airfoil - a poor location for producing lift. This would indicate that the outboard portions of these flap segments did not produce any useful lift.

The foregoing discussion applies to both the 45° and 60° wings, and since the aggregate flap area for both the three-step and six-step arrangements was little different from that of the conventional split flap it appears that the effect of flap area can be eliminated.

Slotted flaps.- The slotted flap produced the largest increase in maximum lift coefficient on both wings. Table III reveals that with the exception of the six-step flap on the 60° wing the slotted flap also produced the largest increment of lift coefficient at $\alpha = 0°$. The largest value of $(L/D)_{max}$ was obtained with the slotted flap. The ratio $(L/D)C_{L_{max}}$ was considerably lower than that for any of the split-flap arrangements except on the 60° wing. Figures 11 and 16

indicate the angle of stall was not appreciably reduced for either wing. The maximum-lift-coefficient increments are plotted in figures 18 and 19. It is noted that the optimum flap angle is 45° for the 45° wing and between 15° and 30° for the 60° wing.

An indication of the drag increase due to flap deflection is given in figures 20 and 21.

As shown in figure 11, a large increase in the pitching-moment coefficients, along with an increase in stability, occurred when the flap was deflected on the 45° wing. A greater increase in stability is noted for the 60° wing in figure 16, but the pitching-moment coefficients are much smaller.

Table III gives an indication of the relative glide angle as compared with other flap arrangements.

Rotated slotted flap.- The rotated slotted flap, pictured in figures 4 and 5 and shown schematically in figures 6 and 7, had its sweep angle reduced by approximately 7° on each wing. From simple sweep theory, it would appear that some gain in lift effectiveness should be realized, but figures 12 and 17 show this flap to be inferior to the conventional slotted flap. In part, this may be due to the fact that the reduction in sweep angle was small, and the point about which the hinge axis was rotated was the outboard end of the flap hinge axis, which was coincident with the 70 percent chord. Since the gap at the inboard end was quite large, it is possible that this, coupled with interference at the outboard section, may have reduced the flap effectiveness. There is a difference of approximately 0.12 in $\Delta C_{L_{max}}$ as compared with the conventional slotted flap (table III). The rotated flap gave very nearly the same glide angle, but $(L/D)_{max}$ was reduced considerably.

The same general effect on the pitching-moment curve is noted, that is, a large negative increase in $C_{m_{c/4}}$. The effect on stability appears to be very nearly the same as that for the slotted flap. A larger increase in slope $\frac{dC_{m_{c/4}}}{dC_L}$ is noted for the 60° wing, however.

The lift and drag increments, $\Delta C_{L_{max}}$ and ΔC_D, are given in figures 18 to 21.

CONCLUSIONS

The results of tests at low speeds of two sweptback wings equipped with several different trailing-edge flaps indicate that for the configurations tested:

1. The effectiveness of the plain split flap is reduced with increasing sweepback. At 60° sweepback no appreciable gain in lift is realized with the split flap.

2. The segmented flaps are even less effective than the plain split flap. It appears that incorporation of such flaps would not be feasible.

3. The slotted flap proved to be the most effective type of high-lift device tested. It retains the disadvantage of causing large diving moments to be developed.

4. Reducing the sweep angle of the slotted flap by the method described herein is of no practical value.

5. Deflection of the flaps increased the lift coefficients at which the wings became unstable but did not reduce the aerodynamic-center shift over the entire lift-coefficient range. Over the stable range of lift coefficients the pitching moments were increased negatively as on straight wings.

6. Only in cases of the split flap and the three-step flap on the 45° wing and the six-step flap on the 60° wing was the glide angle at maximum lift coefficient reduced below that of the plain wing.

7. In general, the effects of the flaps were the same as those on straight wings, except for the decreased effectiveness. The flaps in some instances gave lower drag coefficients and smaller glide angles at maximum lift coefficient than were obtained for the straight wings.

Georgia Institute of Technology
Atlanta, Ga., October 6, 1950

REFERENCES

1. Jones, Robert T.: Wing Plan Forms for High-Speed Flight. NACA Rep. 863, 1947. (Formerly NACA TN 1033.)

2. Luetgebrune, H.: Contributions to Sweep-Back Research. Translation No. F-TS-684-RE, Air Materiel Command, Army Air Corps, Dec. 1946.

3. Betz, A., and Busemann, A.: The Present Status of Research on Swept-Back Wings. Translation No. 80, Ga. Inst. of Technology, 1948.

4. Lowry, John G., and Schneiter, Leslie E.: Investigation at Low Speed of the Longitudinal Stability Characteristics of a 60° Swept-Back Tapered Low-Drag Wing. NACA TN 1284, 1947.

5. Letko, William, and Goodman, Alex: Preliminary Wind-Tunnel Investigation at Low Speed of Stability and Control Characteristics of Swept-Back Wings. NACA TN 1046, 1946.

6. Platt, Robert C.: Aerodynamic Characteristics of a Wing with Fowler Flaps including Flap Loads, Downwash, and Calculated Effect on Take-Off. NACA Rep. 534, 1935.

7. Pope, Alan: Wind-Tunnel Testing. John Wiley & Sons, Inc., 1947, pp. 235-241.

8. Thom, A.: Blockage Corrections in a Closed High-Speed Tunnel. R. & M. No. 2033, British A.R.C., 1943.

9. Toll, Thomas A., and Queijo, M. J.: Approximate Relations and Charts for Low-Speed Stability Derivatives of Swept Wings. NACA TN 1581, 1948.

10. Soulé, Hartley A.: Influence of Large Amounts of Wing Sweep on Stability and Control Problems of Aircraft. NACA TN 1088, 1946.

11. Abbott, Ira H., Von Doenhoff, Albert E., and Stivers, Louis S., Jr.: Summary of Airfoil Data. NACA Rep. 824, 1945.

12. Pearson, Henry A., and Anderson, Raymond F.: Calculation of the Aerodynamic Characteristics of Tapered Wings with Partial-Span Flaps. NACA Rep. 665, 1939.

TABLE I

ORDINATES OF NACA 65A006 AIRFOIL

[Stations and ordinates in percent chord]

Station	Ordinate
0	0
.5	±.464
.75	.563
1.25	.718
2.5	.981
5.0	1.313
7.5	1.591
10	1.824
15	2.194
20	2.474
25	2.687
30	2.842
35	2.945
40	2.996
45	2.992
50	2.925
55	2.793
60	2.602
65	2.364
70	2.087
75	1.775
80	1.437
85	1.083
90	.727
95	.370
100	.013
L.E. radius:	0.229
T.E. radius:	0.014



TABLE II

PRESENTATION OF RESULTS

(a) Results for various flap configurations

Figure	Configuration	Dynamic pressure q	Data plotted
	$\Lambda = 45^\circ$		
8	Split flap	36.5	C_L against α
9	Three-step flap	36.5	C_D, $C_{m_{c/4}}$ against C_L
10	Six-step flap	36.5	
11	Slotted flap	36.5	
12	Rotated slotted flap	36.5	
	$\Lambda = 60^\circ$		
13	Split flap	30.5	C_L against α
14	Three-step flap	25.6	C_D, $C_{m_{c/4}}$ against C_L
15	Six-step flap	36.5	
16	Slotted flap	25.6	
17	Rotated slotted flap	25.6	

(b) Special plots

Figure	Data plotted
18 - $\Delta C_{L_{max}}$ due to flaps, 45° wing	$\Delta C_{L_{max}}$ against δ_f
19 - $\Delta C_{L_{max}}$ due to flaps, 60° wing	$\Delta C_{L_{max}}$ against δ_f
20 - ΔC_D due to flaps, 45° wing	ΔC_D against δ_f at constant C_L
21 - ΔC_D due to flaps, 60° wing	ΔC_D against δ_f at constant C_L
22 - Tuft studies, 45° and 60° wing	
23 - Aerodynamic-center shift, 45° and 60° wing	Aerodynamic-center position against C_L
25 - ΔC_L against Λ for split flap only, 45° and 60° wing	ΔC_L against Λ ($\alpha = 0$) $\Delta C_{L_{max}}$ against Λ

TABLE III

AERODYNAMIC DATA

Configuration	δ_f for $C_{L_{max}}$ (deg) (a)	$C_{L_{max}}$	$(\Delta C_L)_{\alpha=0}$ (for $\delta_f = 60°$)	C_D at $C_{L_{max}}$ (b)	L/D at $C_{L_{max}}$ (b)	Glide angle at $C_{L_{max}}$ (deg) (b)	$(L/D)_{max}$ (b)
45° wing							
Plain wing	--	1.03	----	0.505	2.04	26.1	21.3
Split flap	30	1.21	0.50	.565	2.14	25.0	6.05
Three-step flap	30	1.035	.50	.422	2.45	22.4	4.45
Six-step flap	45	1.12	.61	.574	1.95	27.2	3.61
Slotted flap	45	1.62	.72	.943	1.72	30.1	6.47
Rotated slotted flap	45	1.51	.66	.929	1.62	31.6	5.16
60° wing							
Plain wing	---	1.0	----	0.766	1.31	37.3	20.0
Split flap	30	1.05	0.27	.995	1.06	43.3	8.0
Three-step flap	[c]15	1.0	.275	.859	1.16	40.7	7.0
Six-step flap	[c]15	1.0	.42	.732	1.37	36.1	5.3
Slotted flap	15	1.4	.35	1.22	1.15	41.0	10.4
Rotated slotted flap	15	1.27	.23	1.038	1.22	39.3	6.9

[a] Flap deflection giving maximum lift.

[b] Values corresponding to δ_f for $C_{L_{max}}$.

[c] These flaps caused a decrement of $C_{L_{max}}$ at all deflections above 15°.

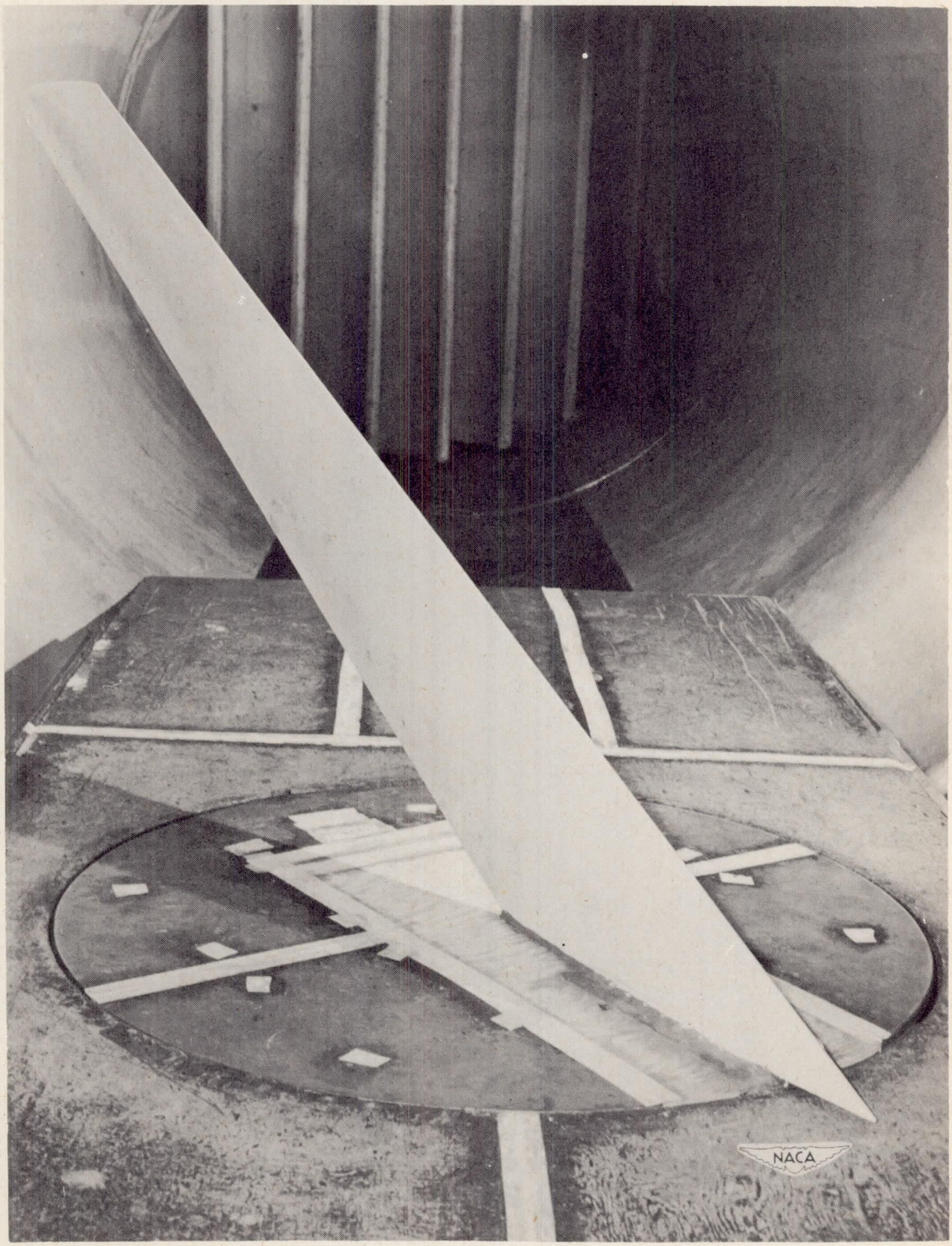


Figure 1.- Photograph of 60° model mounted in tunnel (open jet).

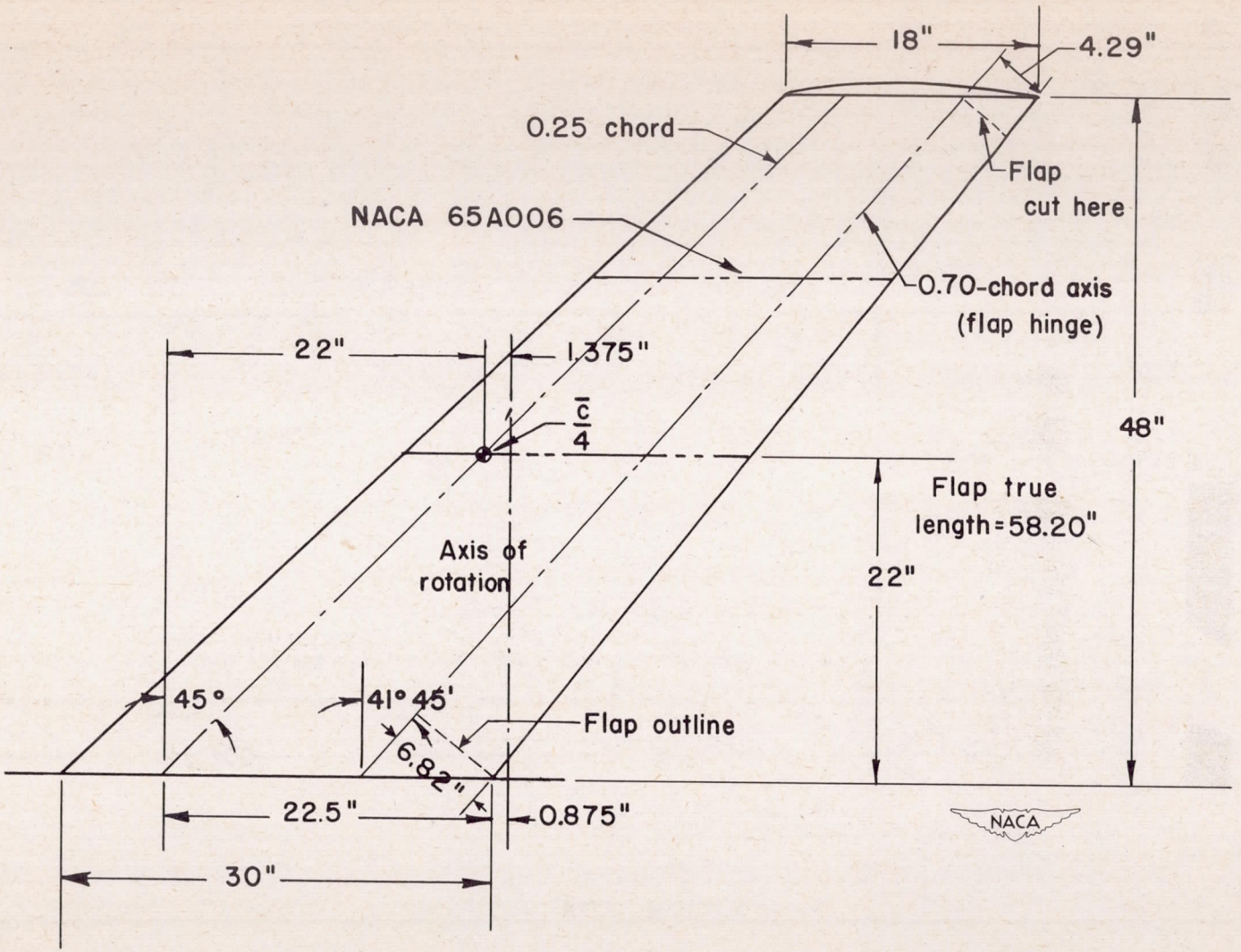


Figure 2.- Plan-form dimensions of 45° swept wing. S = 8 square feet; A = 4; λ = 0.6; $\bar{c}$ = 24.5 inches; all flaps are full-span and are 0.30c.

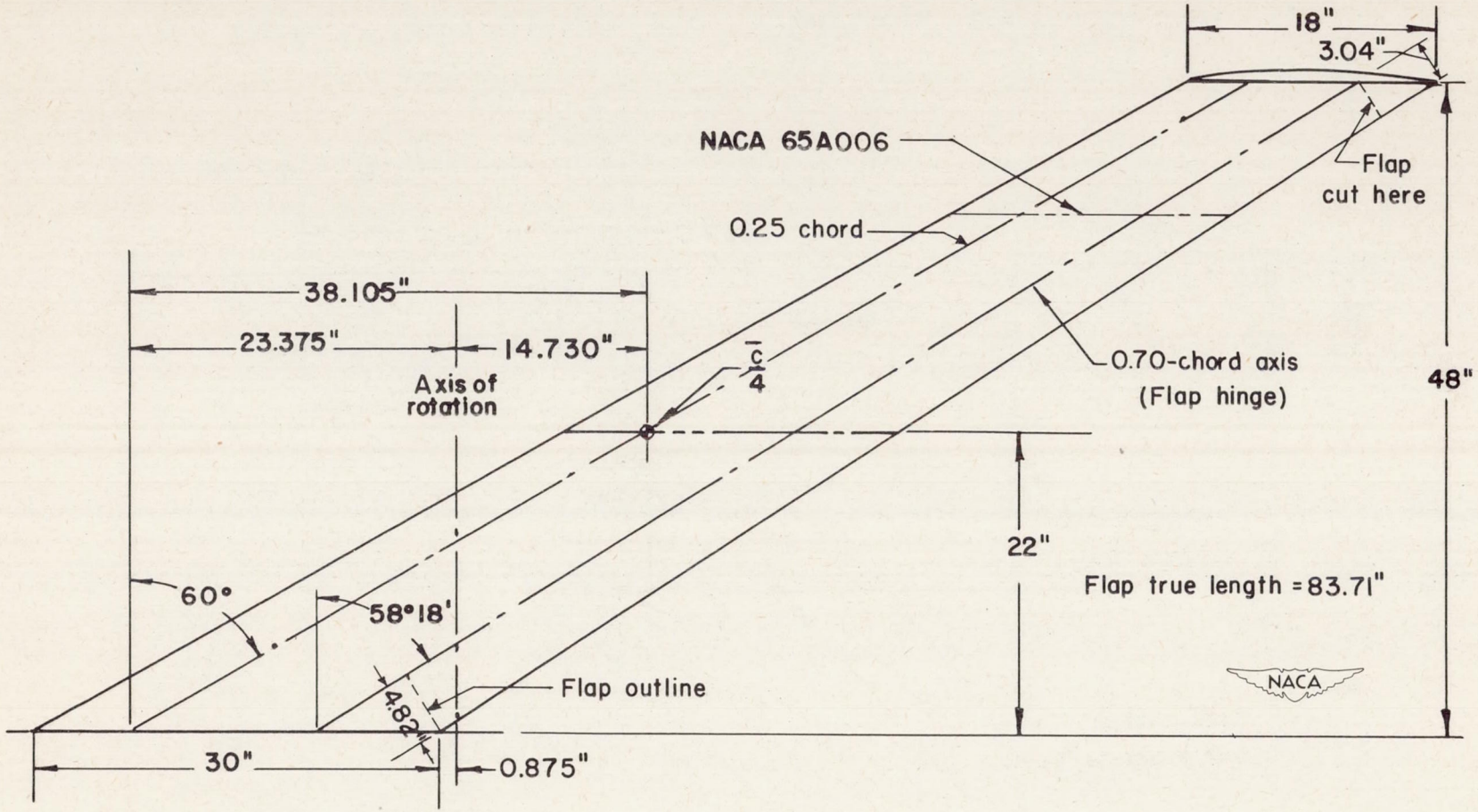
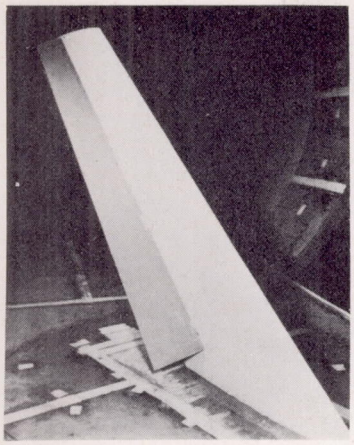
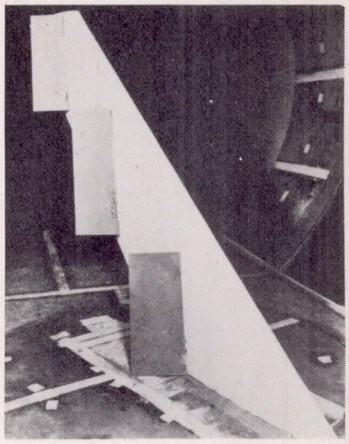


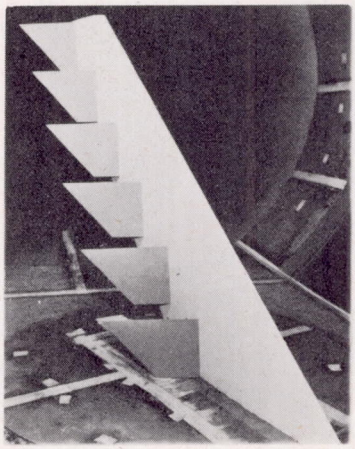
Figure 3.- Plan-form dimensions of 60° swept wing. S = 8 square feet; A = 4; λ = 0.6; $\bar{c}$ = 24.5 inches.



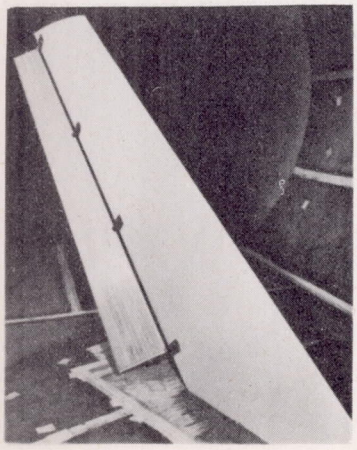
(a) Split flap.



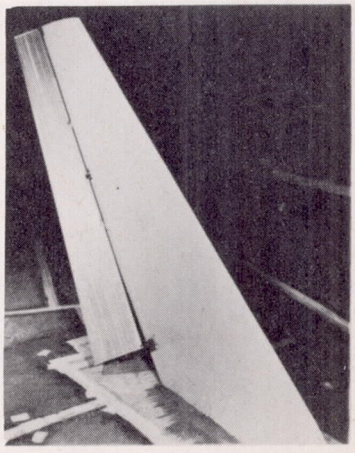
(b) Three-step flap.



(c) Six-step flap.

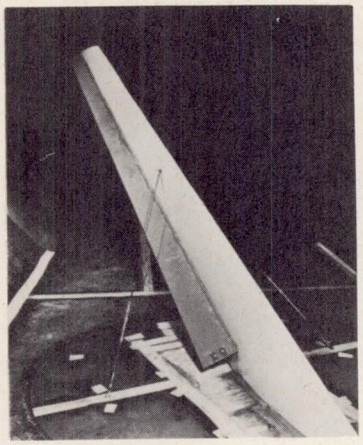


(d) Slotted flap.

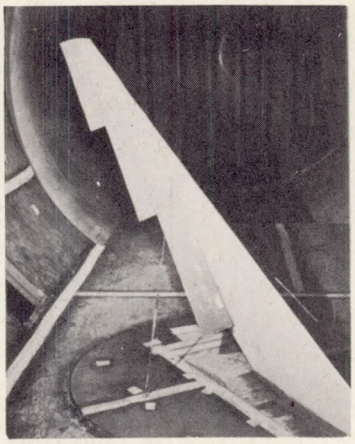


(e) Rotated slotted flap.

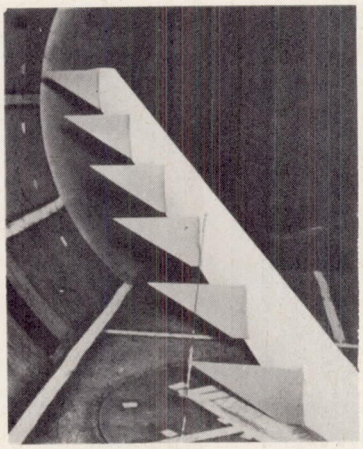
Figure 4.- Flap arrangement - 45° model.



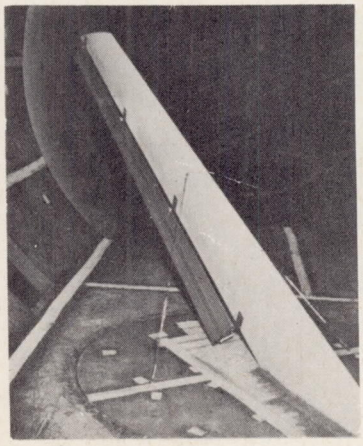
(a) Split flap.



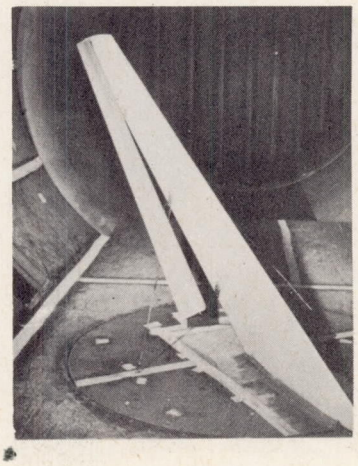
(b) Three-step flap.



(c) Six-step flap.

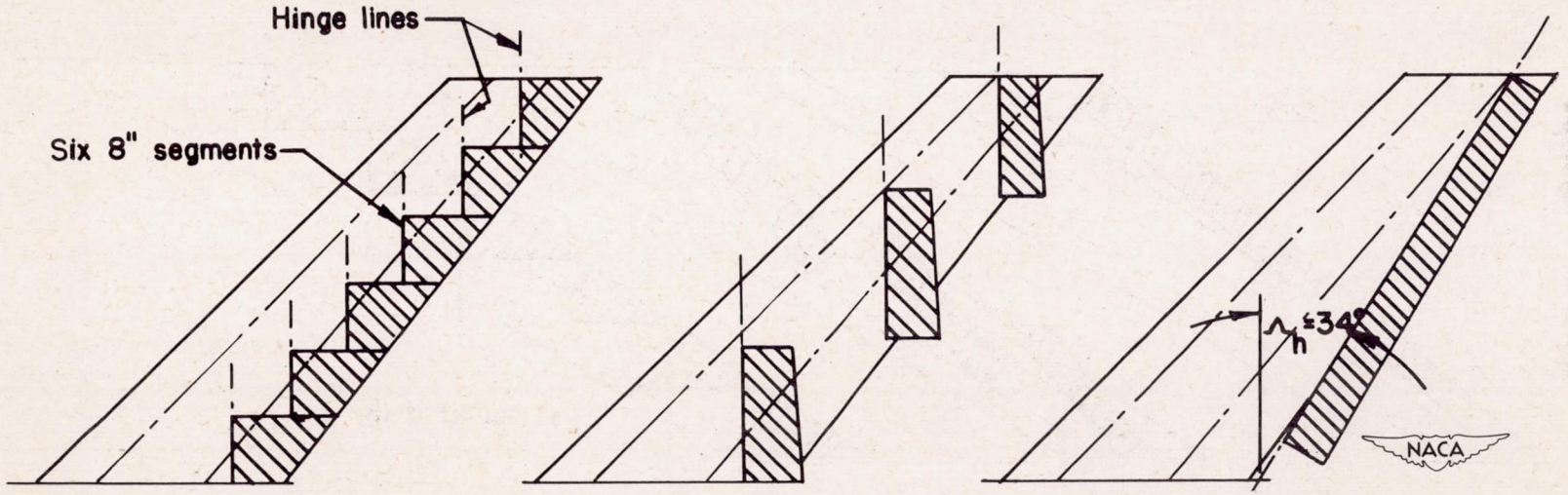


(d) Slotted flap.



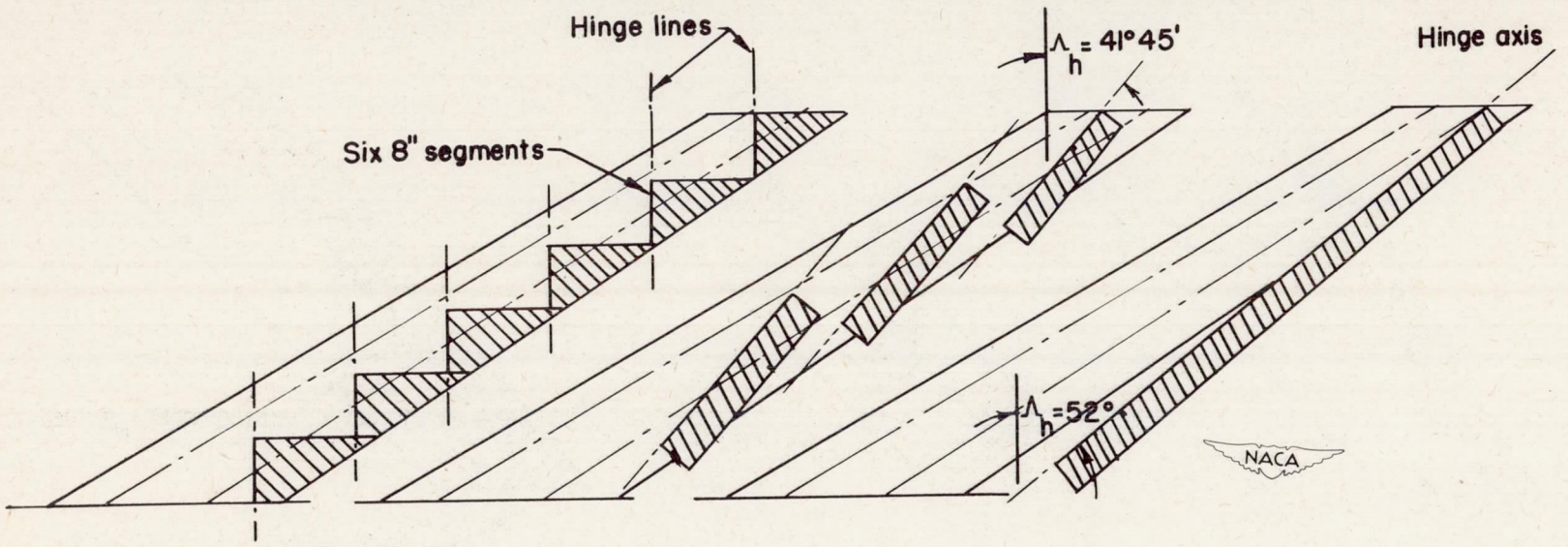
(e) Rotated slotted flap.

Figure 5.- Flap arrangement - 60° model.



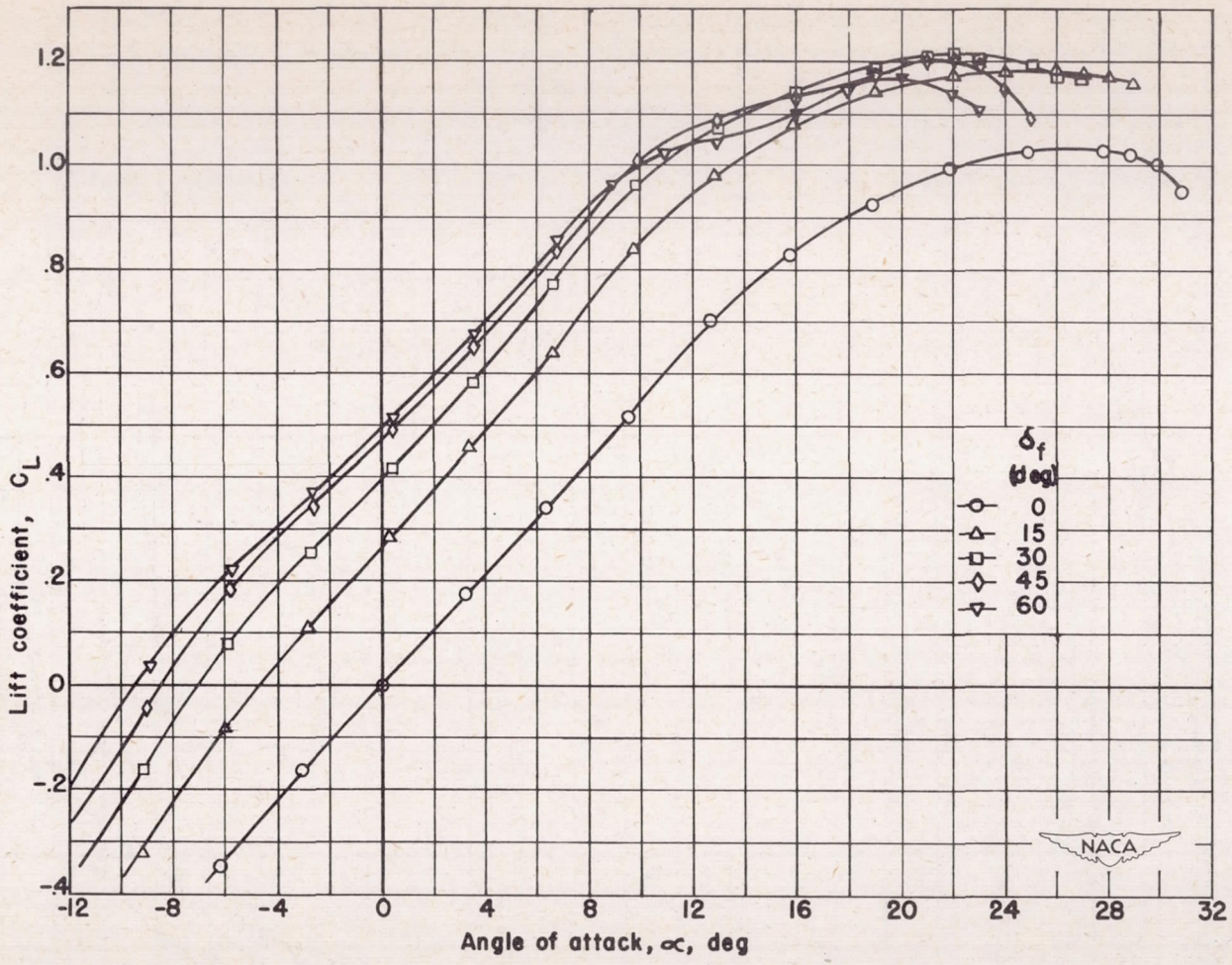
(a) Six-step flap. (b) Three-step flap. (c) Rotated slotted flap.

Figure 6.- Schematic arrangement of special flaps - 45° model.



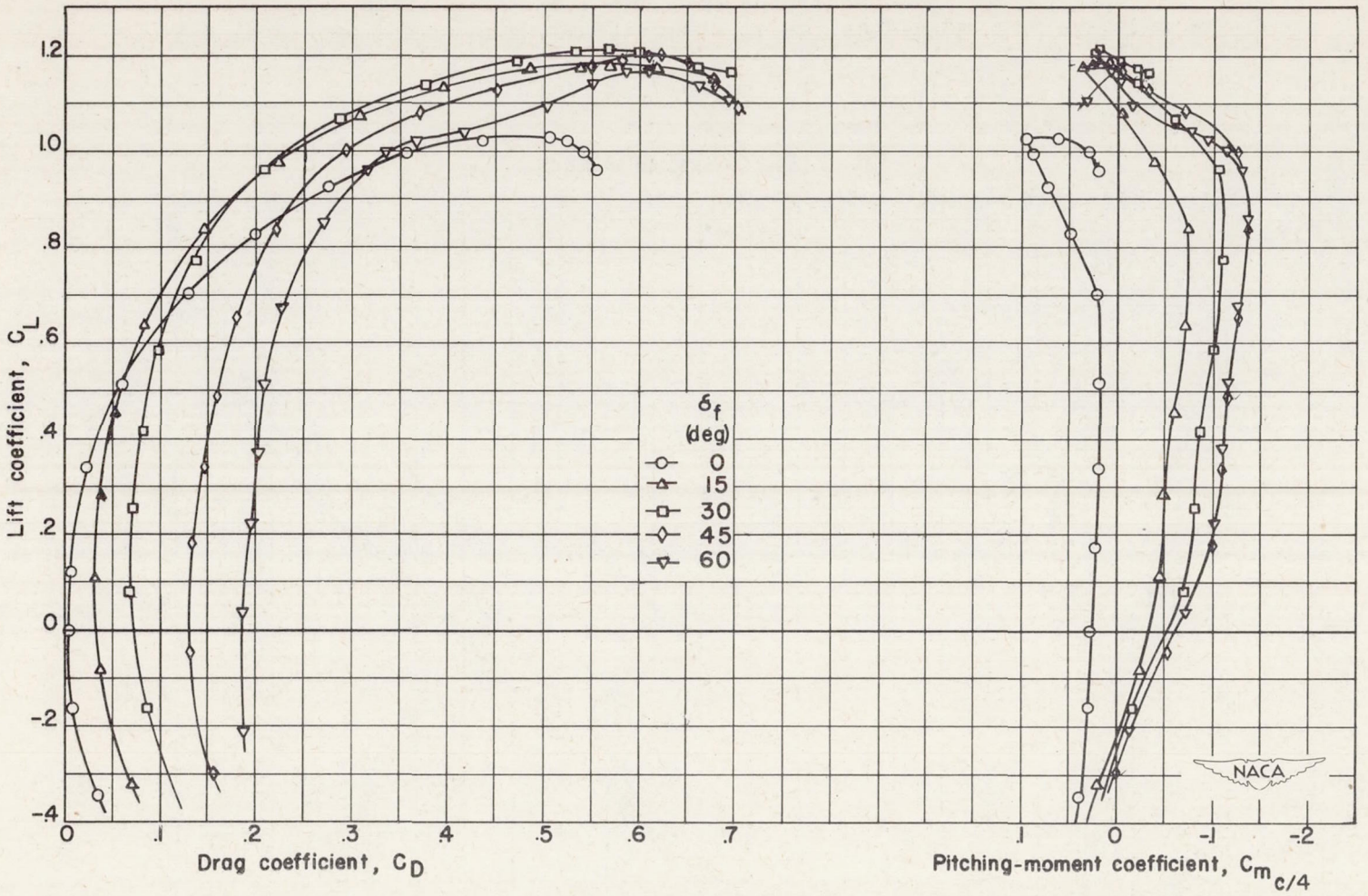
(a) Six-step flap. (b) Three-step flap. (c) Rotated slotted flap.

Figure 7.- Schematic arrangement of special flaps - 60° model.



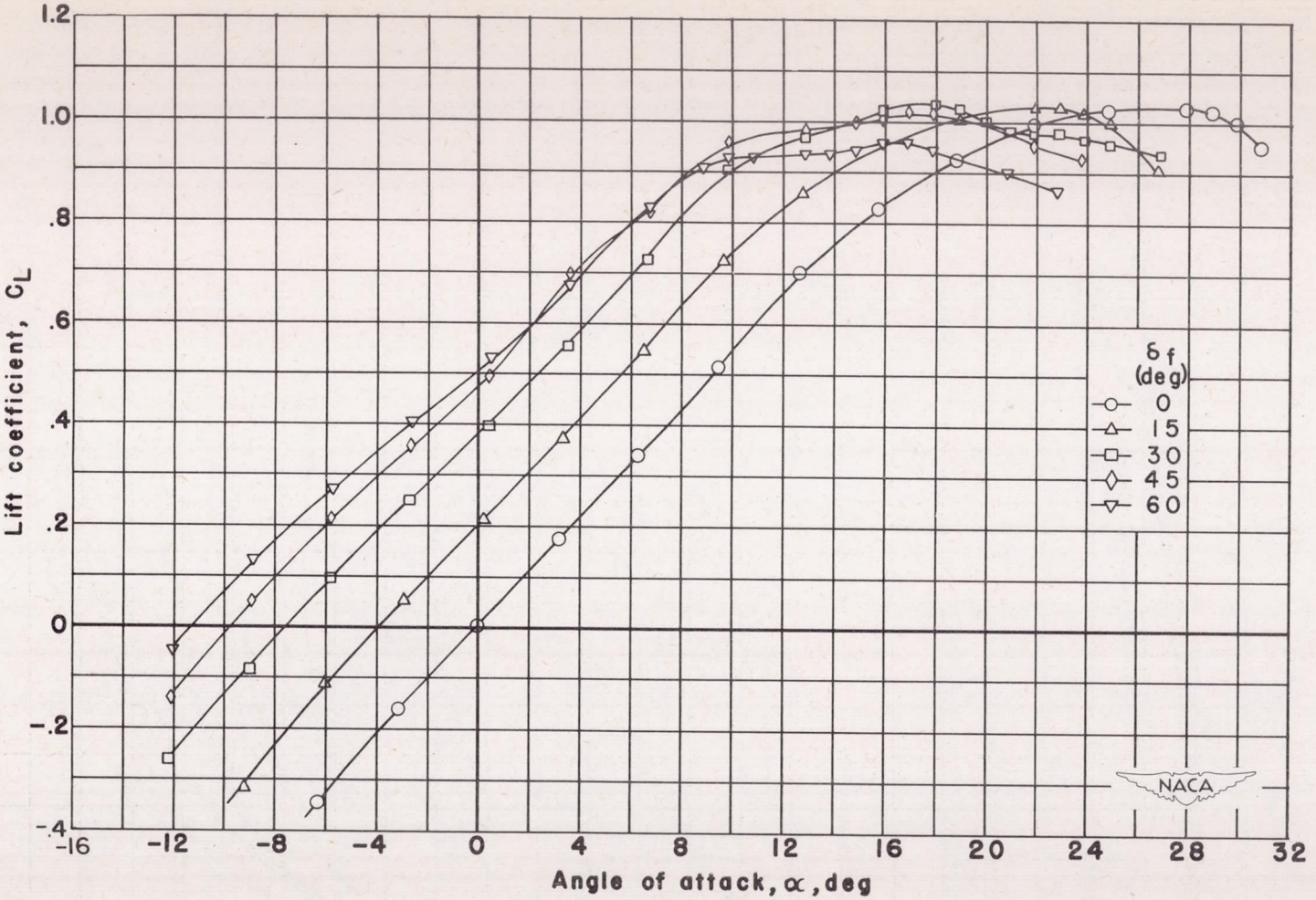
(a) C_L against α.

Figure 8.- Aerodynamic characteristics of 45° sweptback wing with plain split flap. q = 36.5 pounds per square foot.



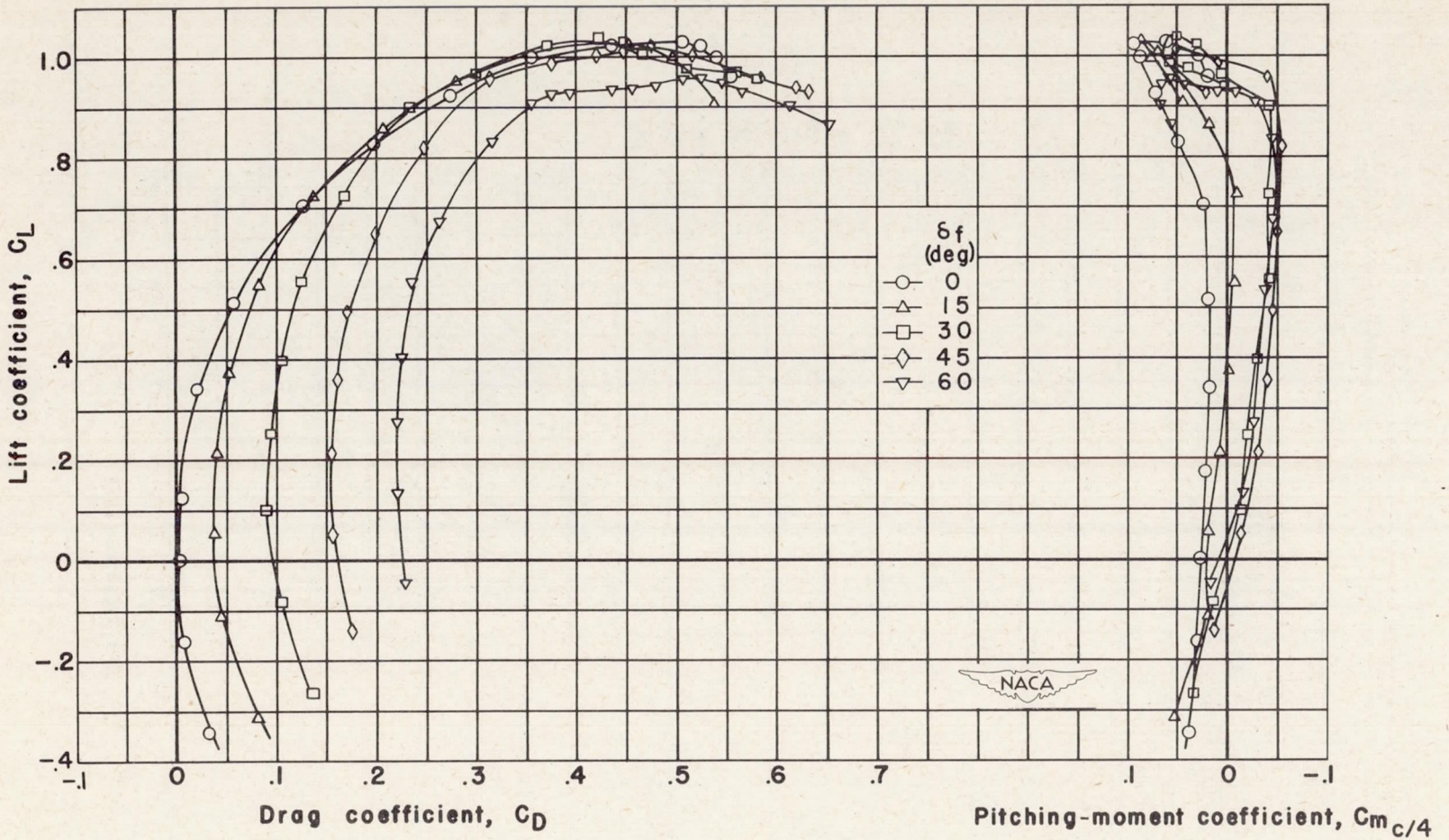
(b) C_L against C_D and $C_{m_{c/4}}$.

Figure 8.- Concluded.



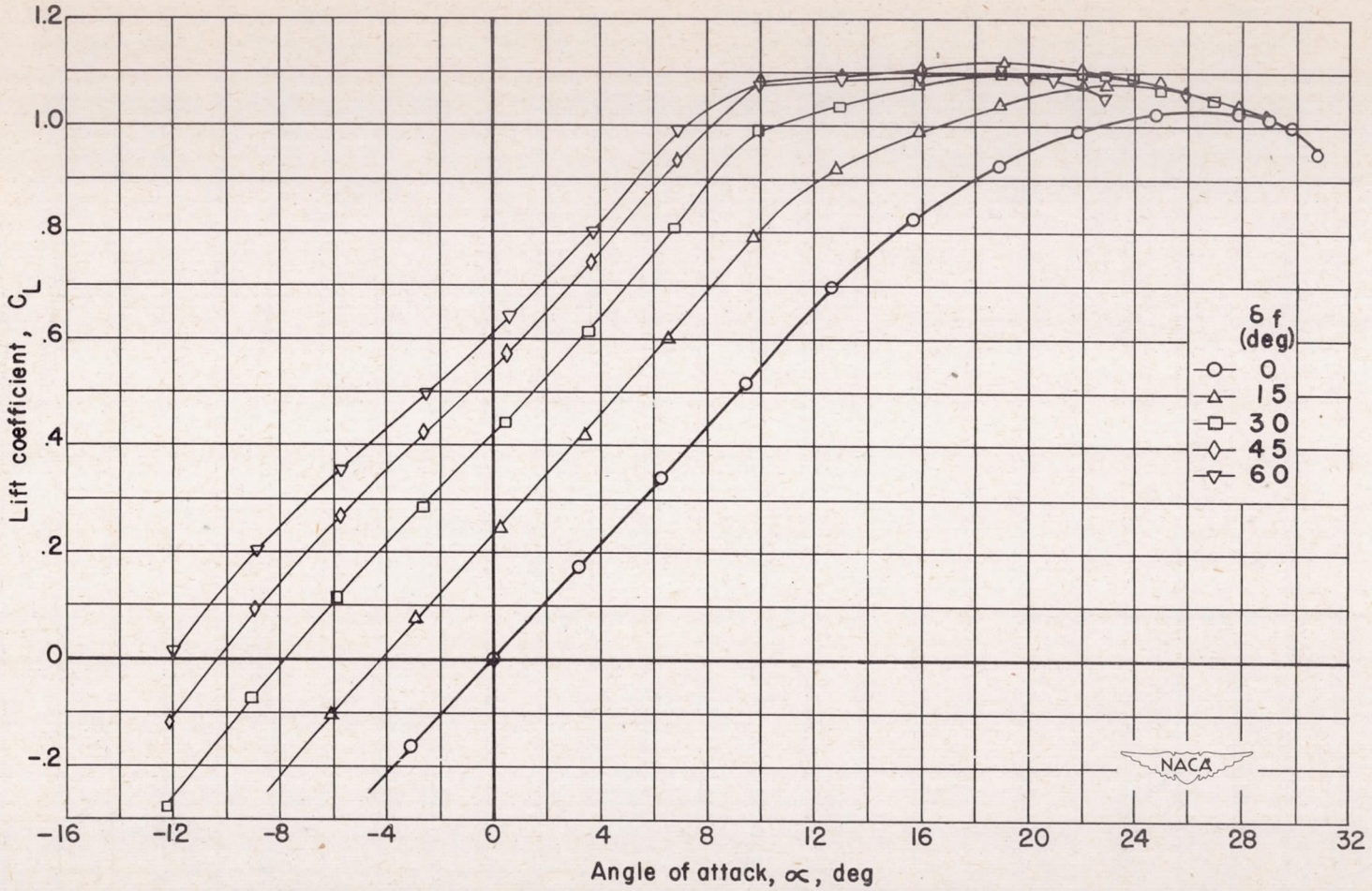
(a) C_L against α.

Figure 9.- Aerodynamic characteristics of 45° sweptback wing with three-step flap. q = 36.5 pounds per square foot.



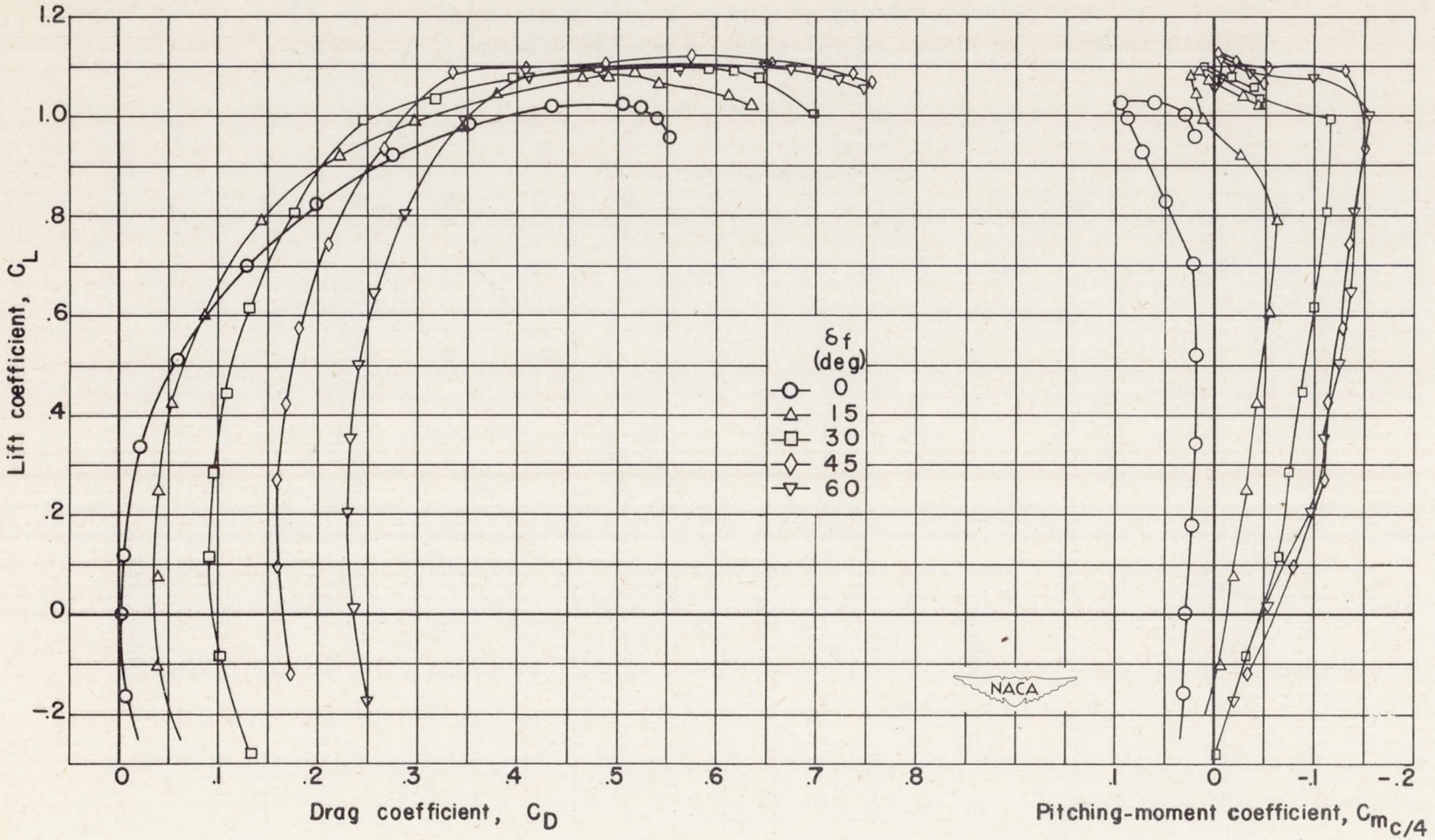
(b) C_L against C_D and $C_{m_{c/4}}$.

Figure 9.- Concluded.



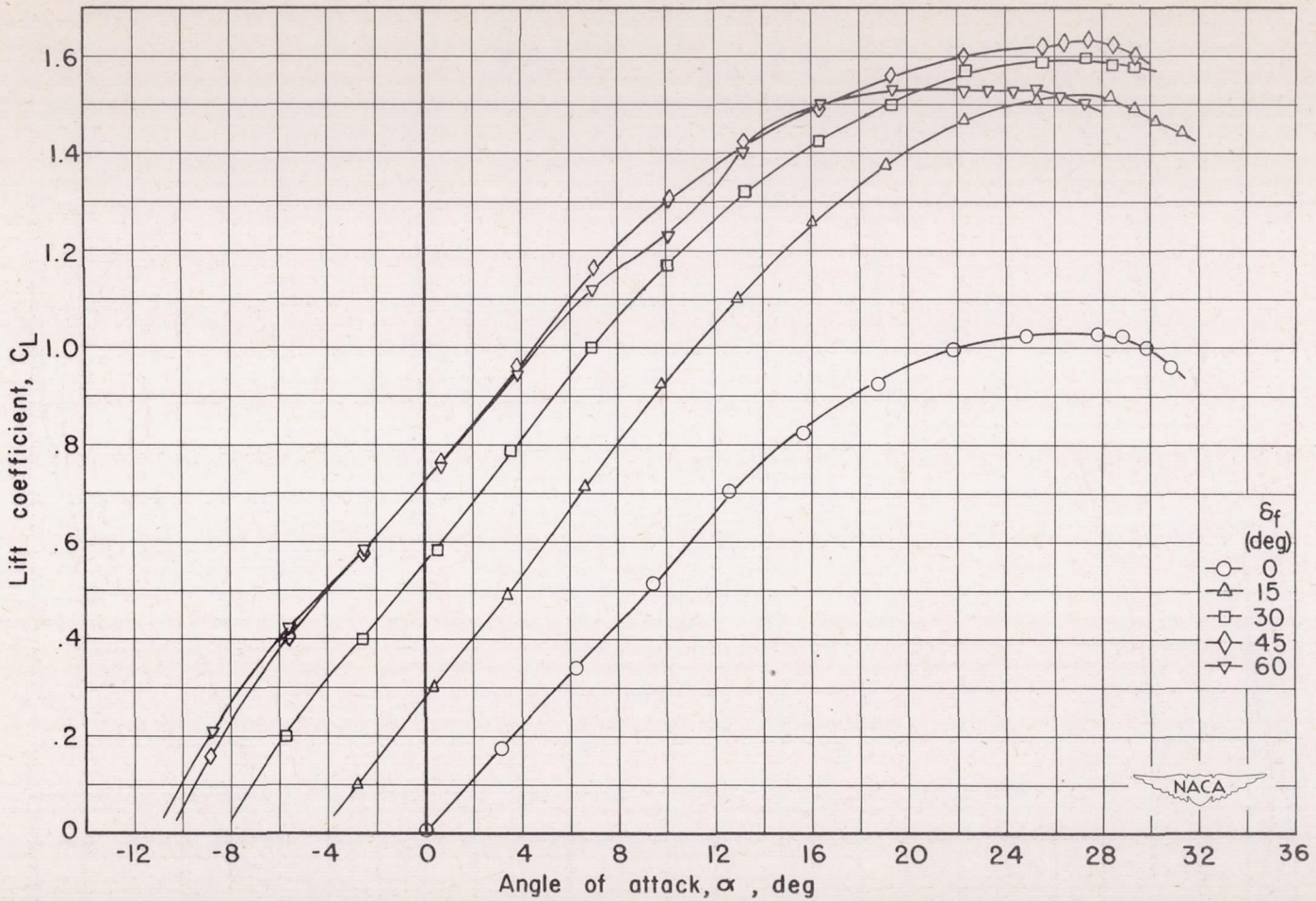
(a) C_L against α.

Figure 10.- Aerodynamic characteristics of 45° sweptback wing with six-step flap. q = 36.5 pounds per square foot.



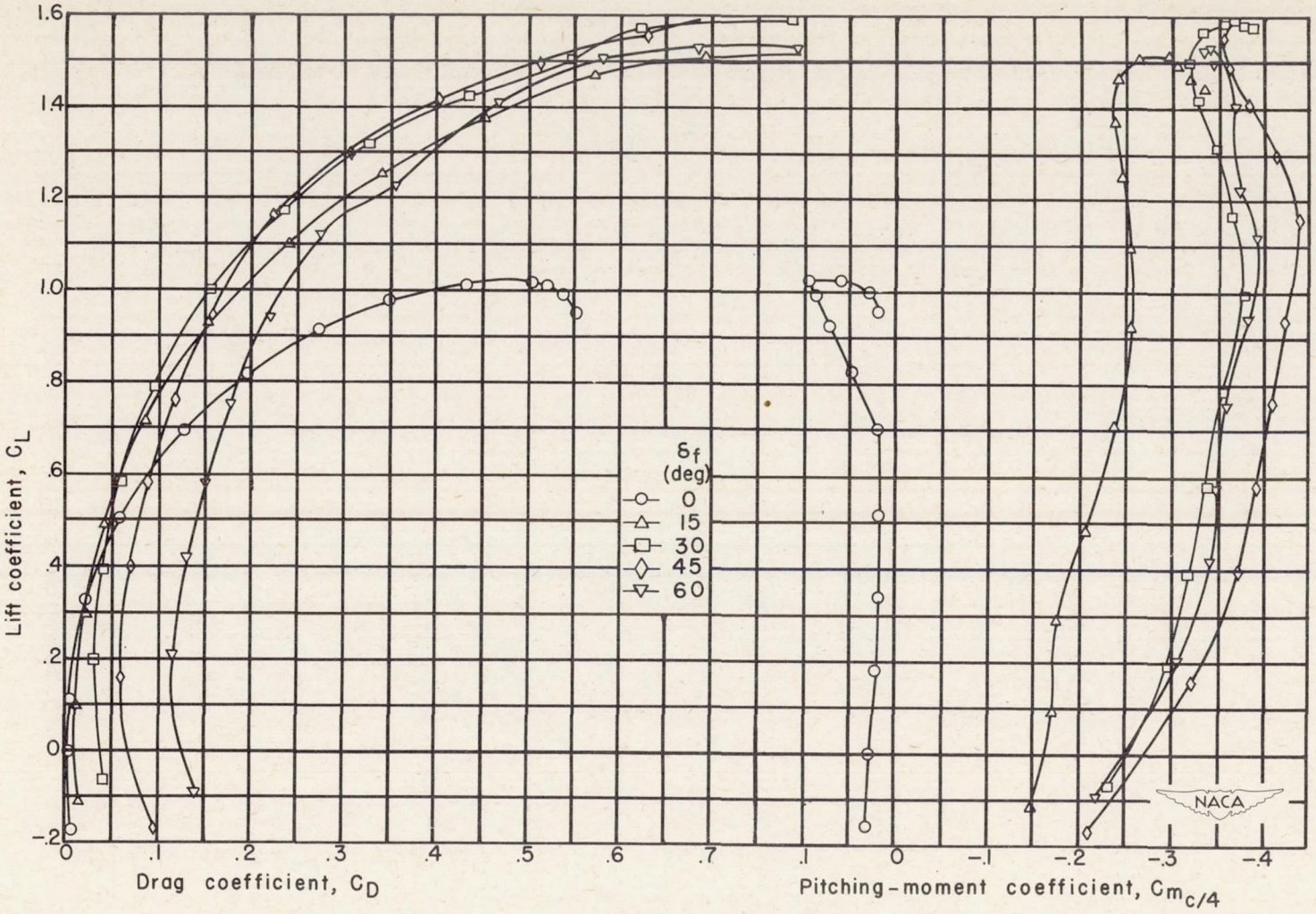
(b) C_L against C_D and $C_{m_{c/4}}$.

Figure 10.- Concluded.



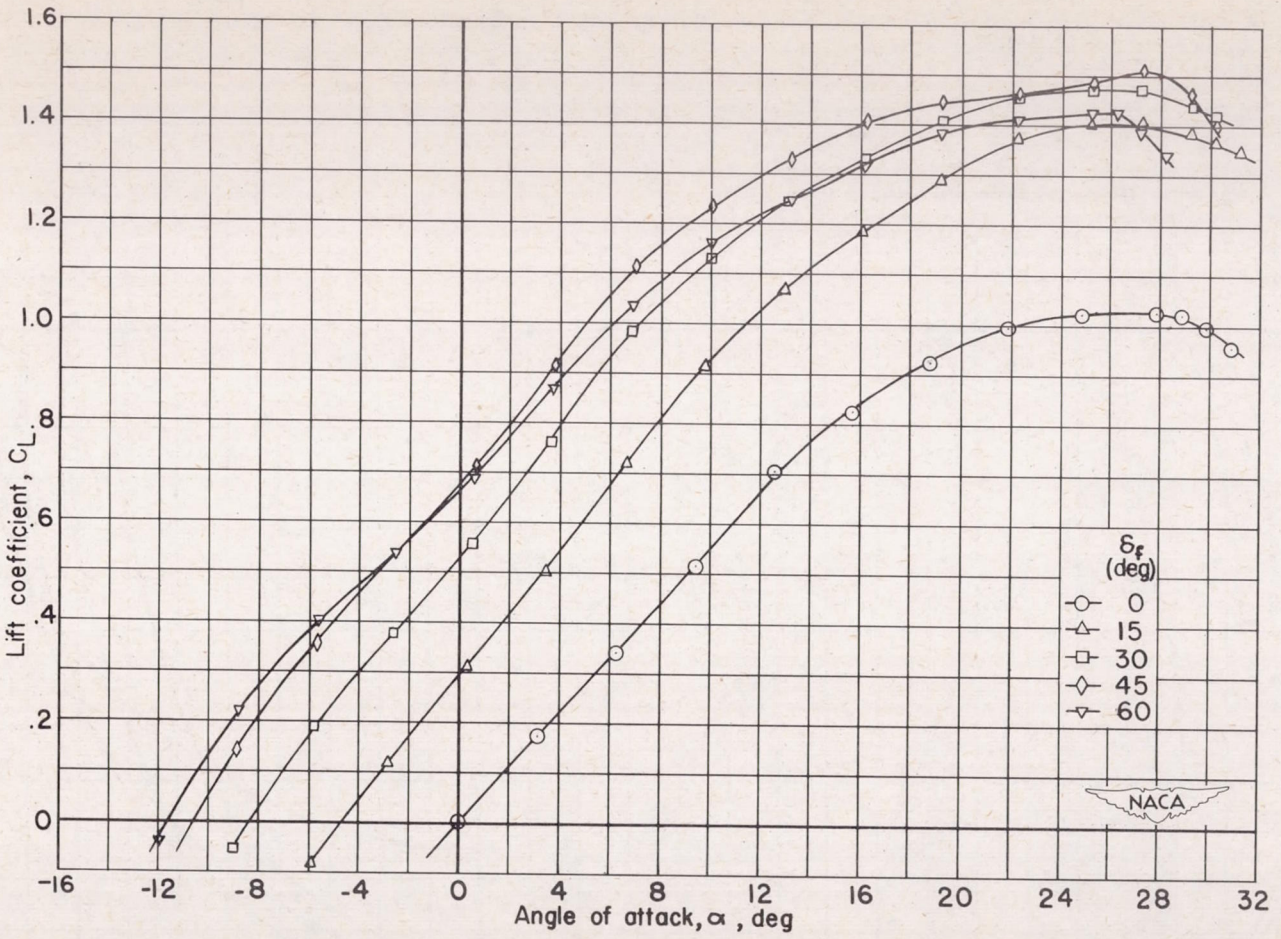
(a) C_L against α.

Figure 11.- Aerodynamic characteristics of 45° sweptback wing with slotted flap. q = 36.5 pounds per square foot.



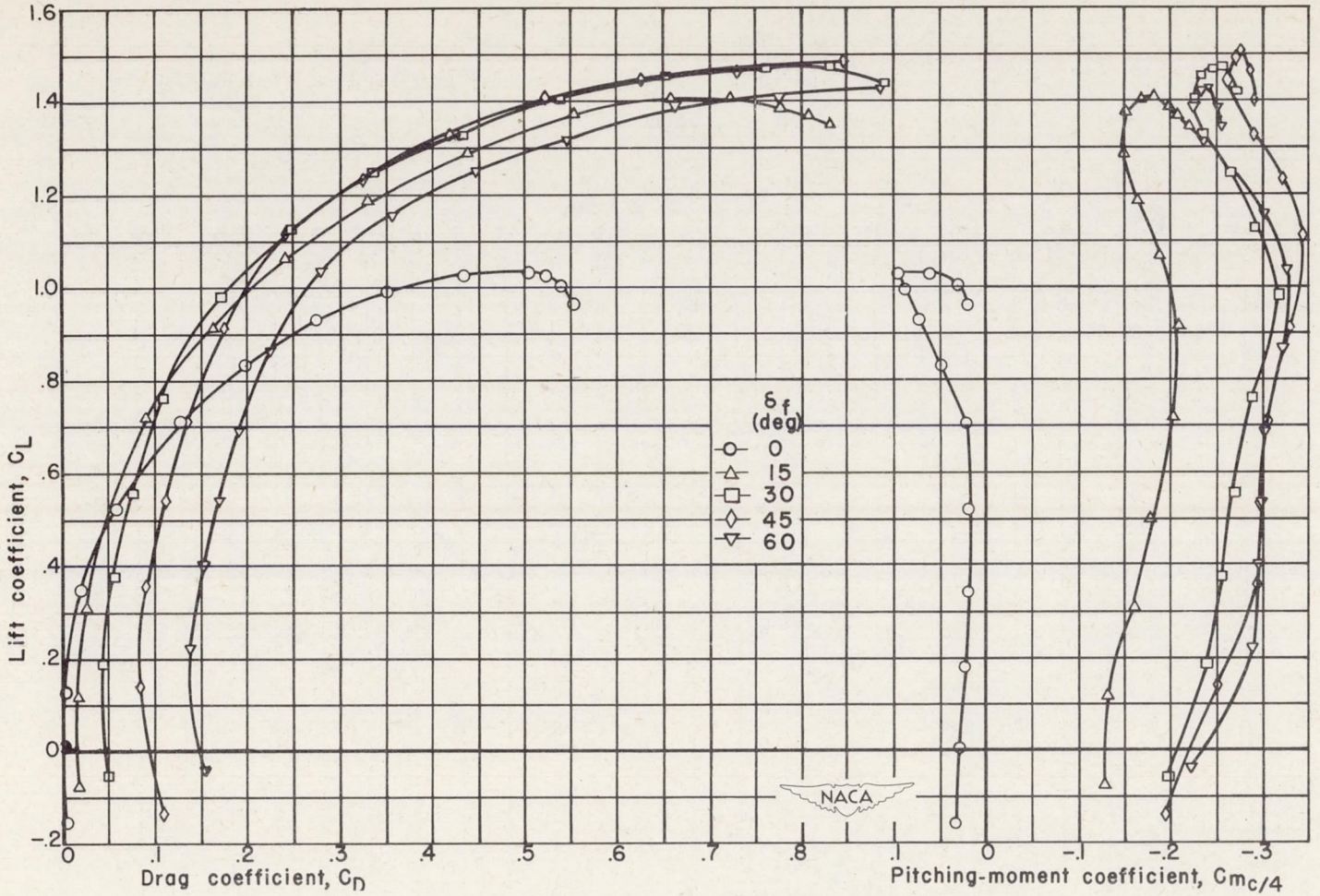
(b) C_L against C_D and $C_{m_{c/4}}$.

Figure 11.- Concluded.



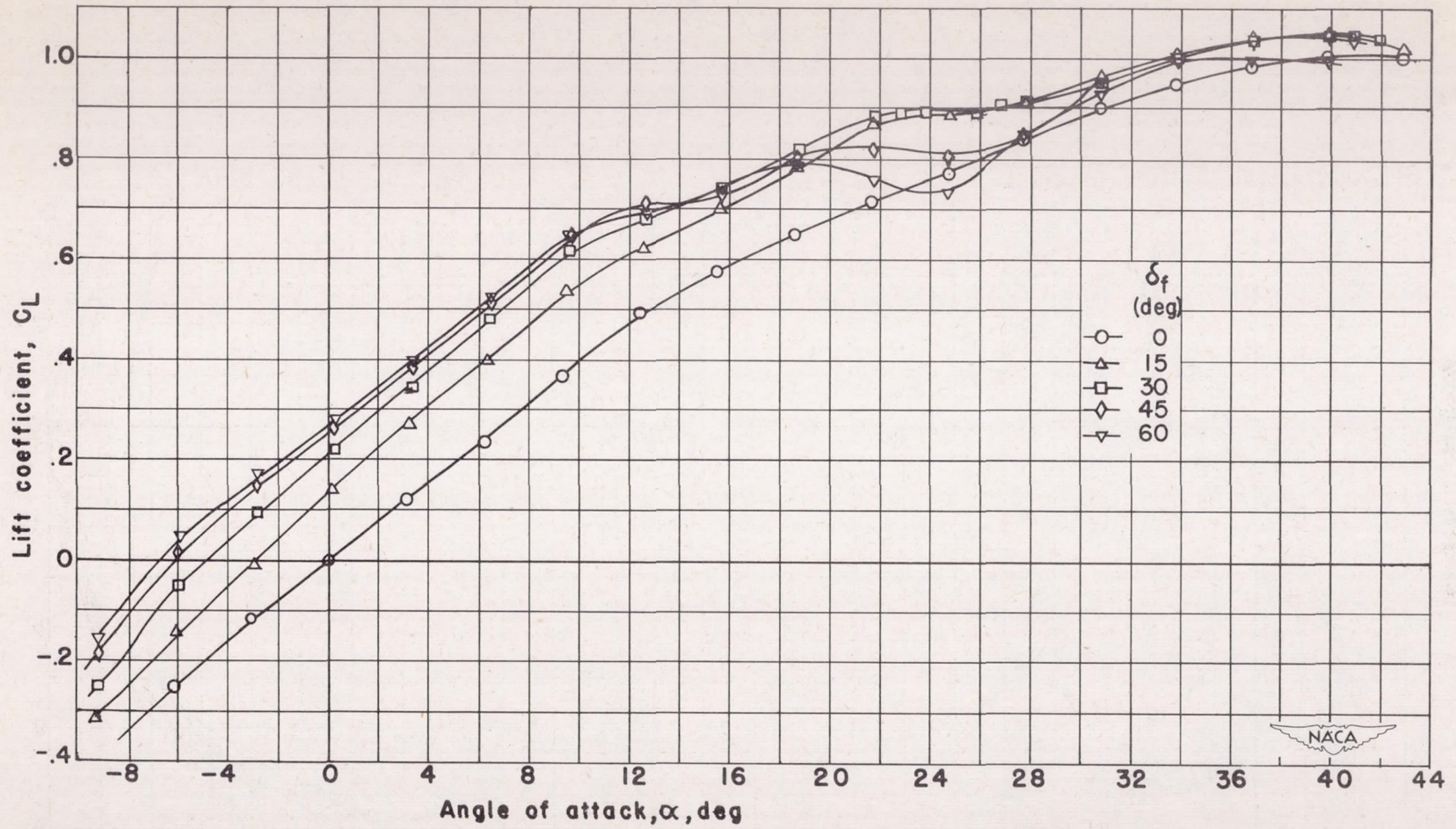
(a) C_L against α.

Figure 12.- Aerodynamic characteristics of 45° sweptback wing with rotated slotted flap. q = 36.5 pounds per square foot.



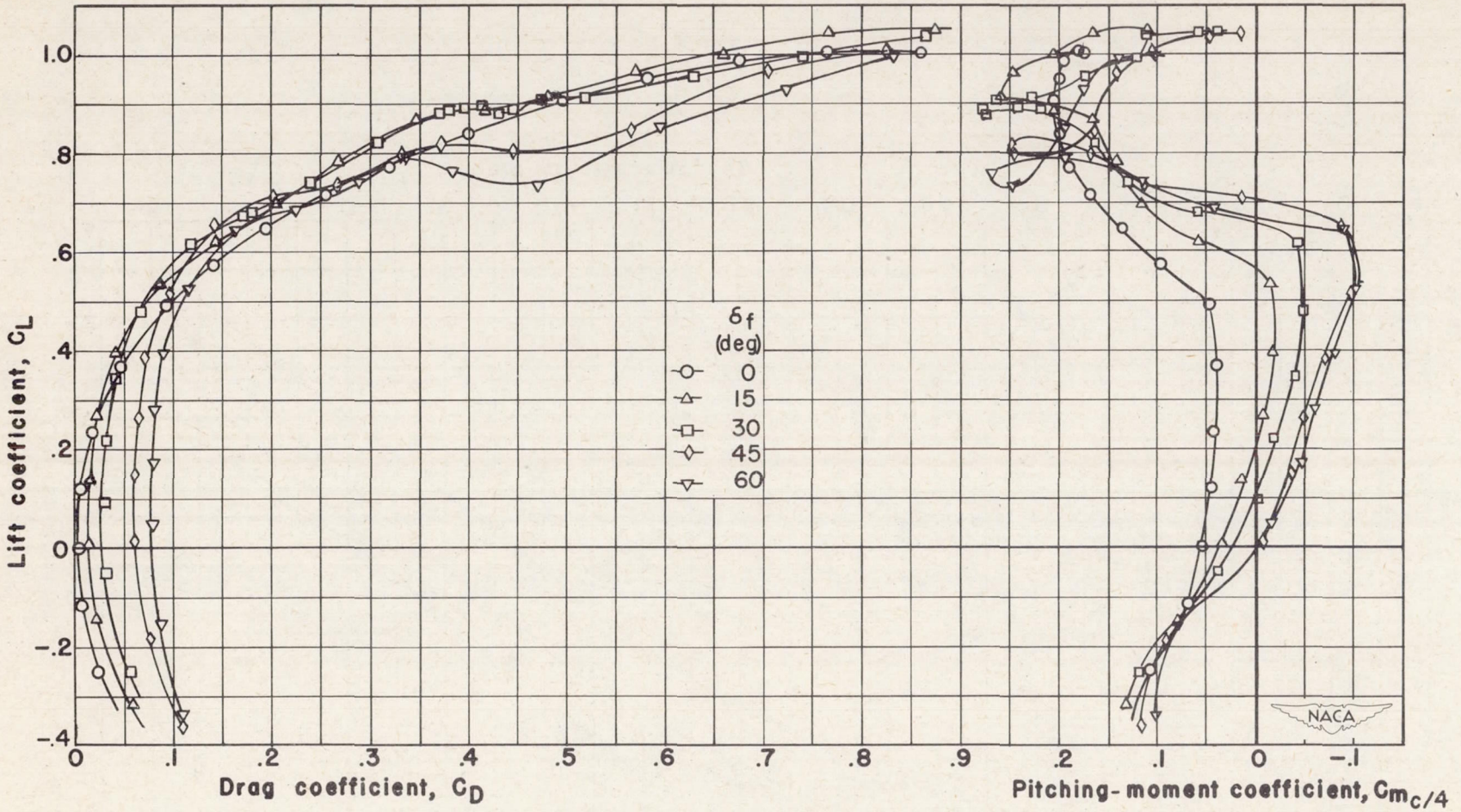
(b) C_L against C_D and $C_{m_{c/4}}$.

Figure 12.- Concluded.



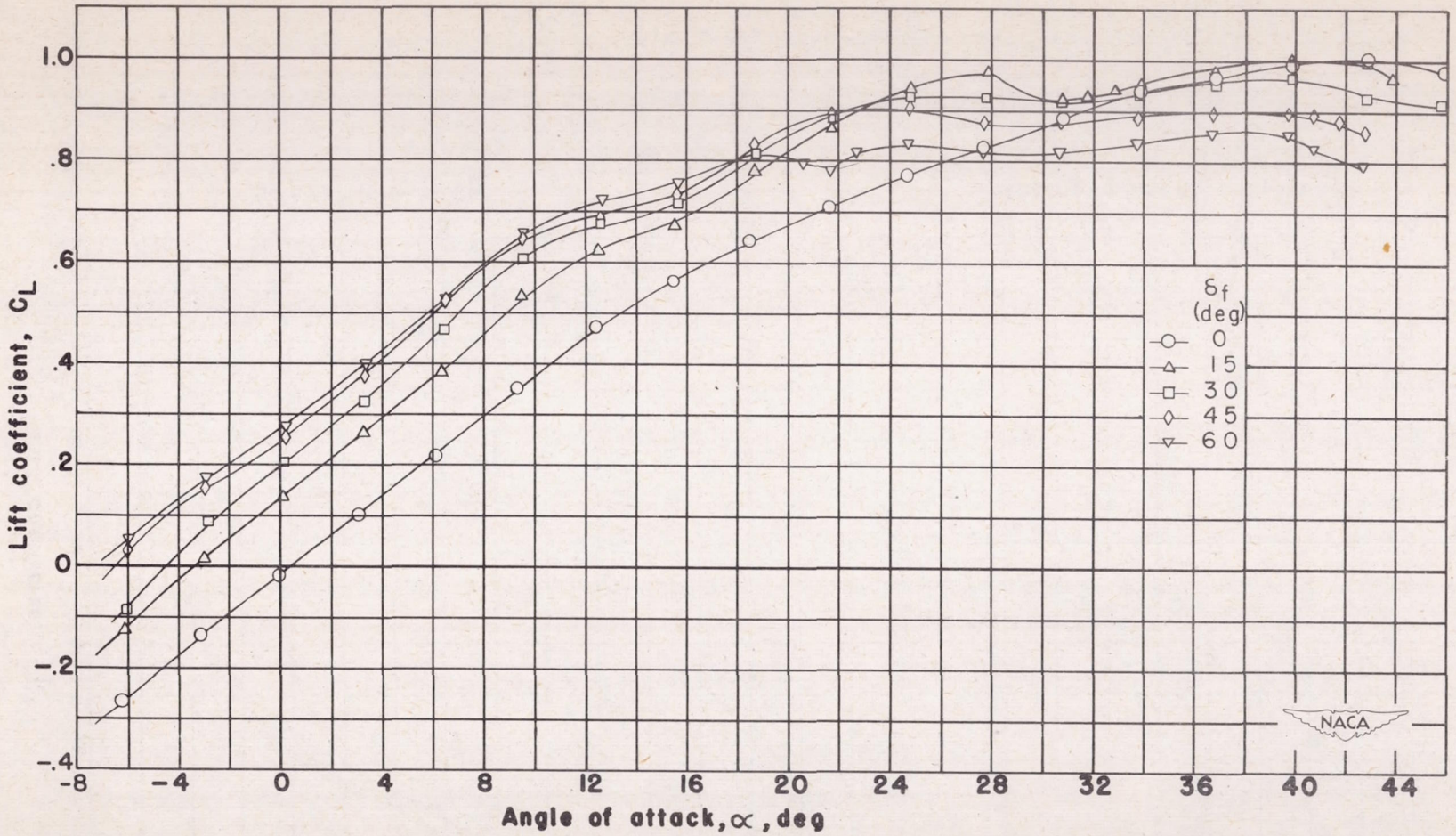
(a) C_L against α.

Figure 13.- Aerodynamic characteristics of 60° sweptback wing with split flap. q = 36.5 pounds per square foot.



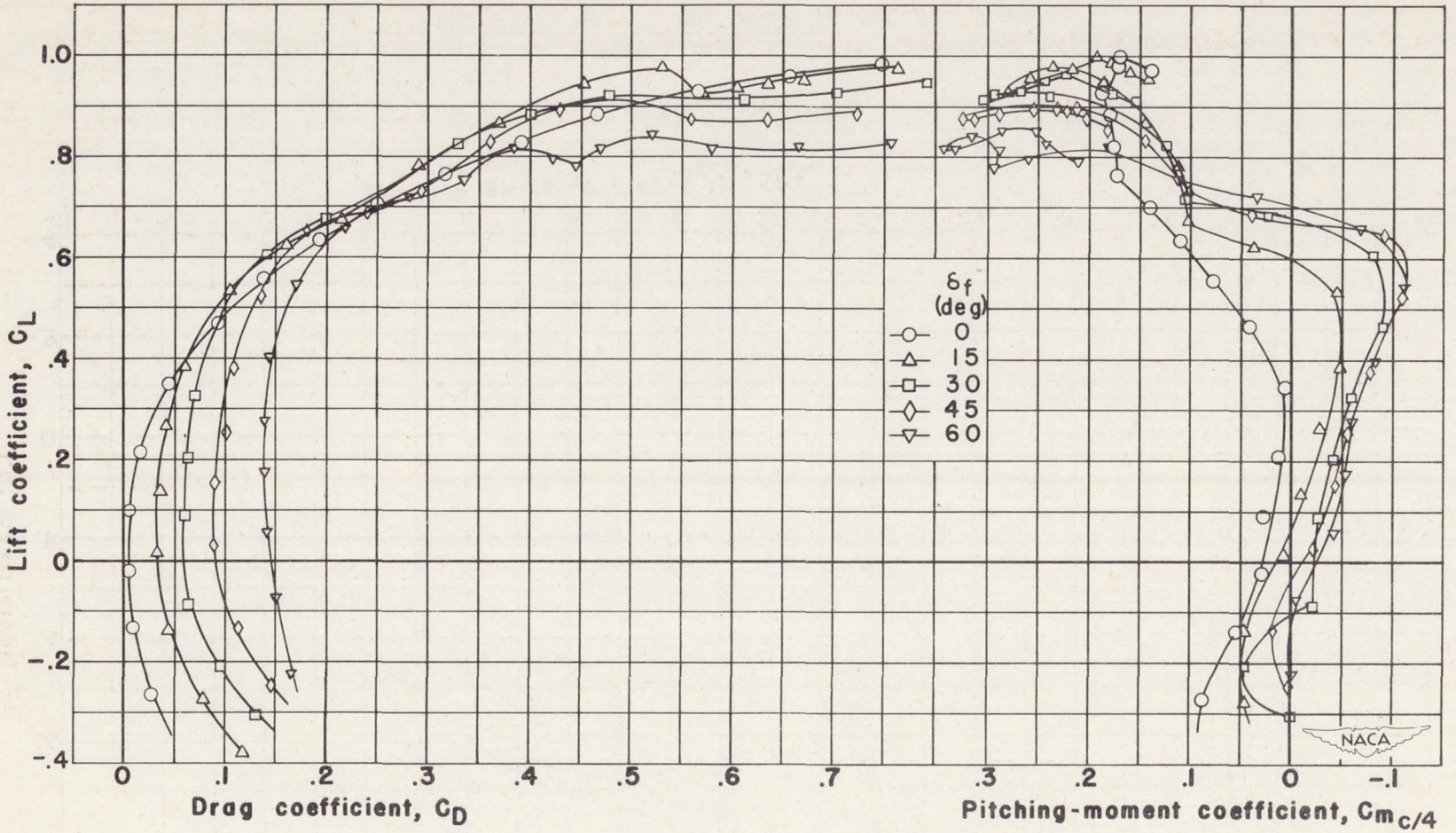
(b) C_L against C_D and $C_{m_{c/4}}$.

Figure 13.- Concluded.



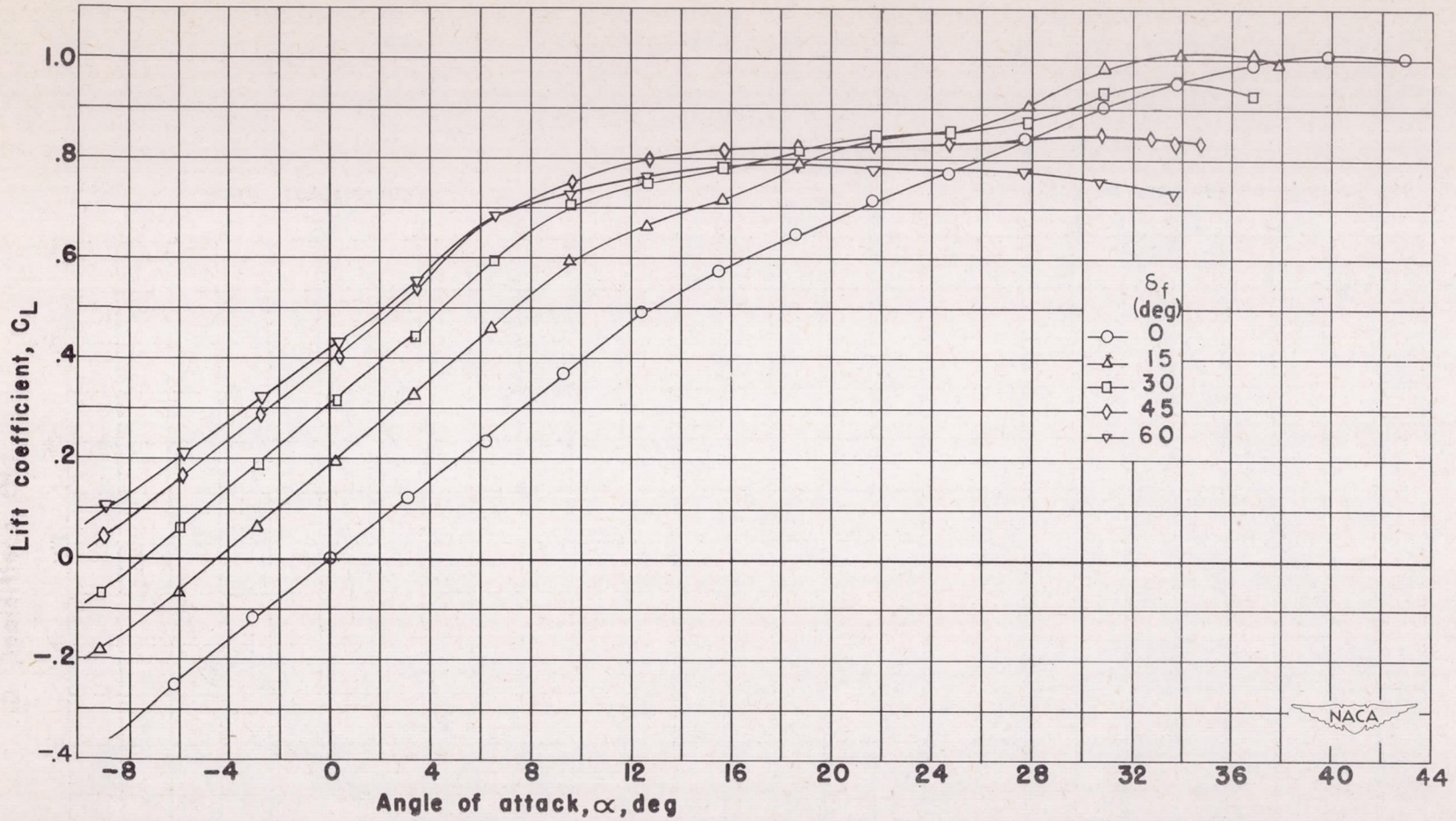
(a) C_L against α.

Figure 14.- Aerodynamic characteristics of 60° sweptback wing with three-step flap. q = 25.6 pounds per square foot.



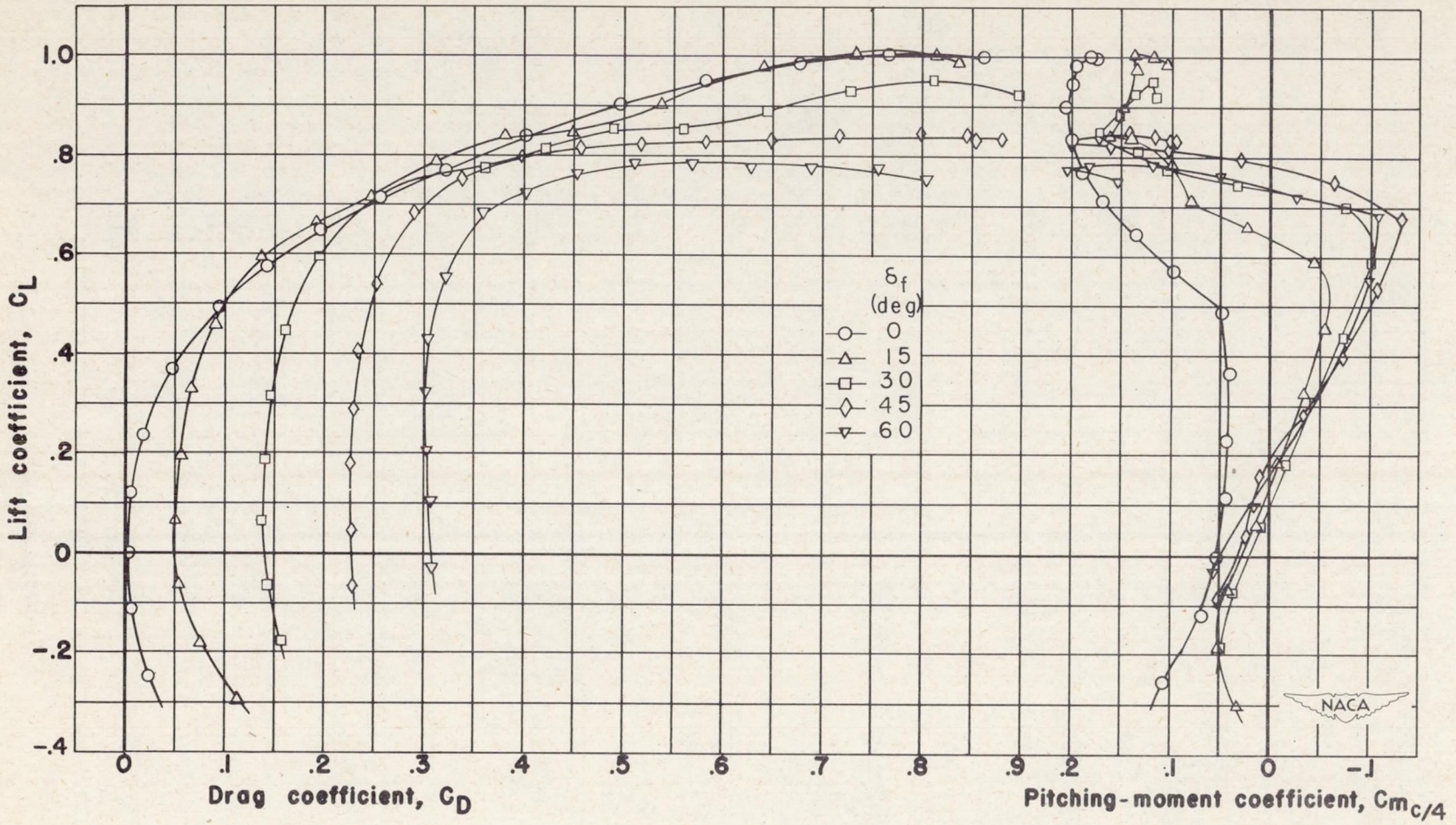
(b) C_L against C_D and $C_{m_{c/4}}$.

Figure 14.- Concluded.



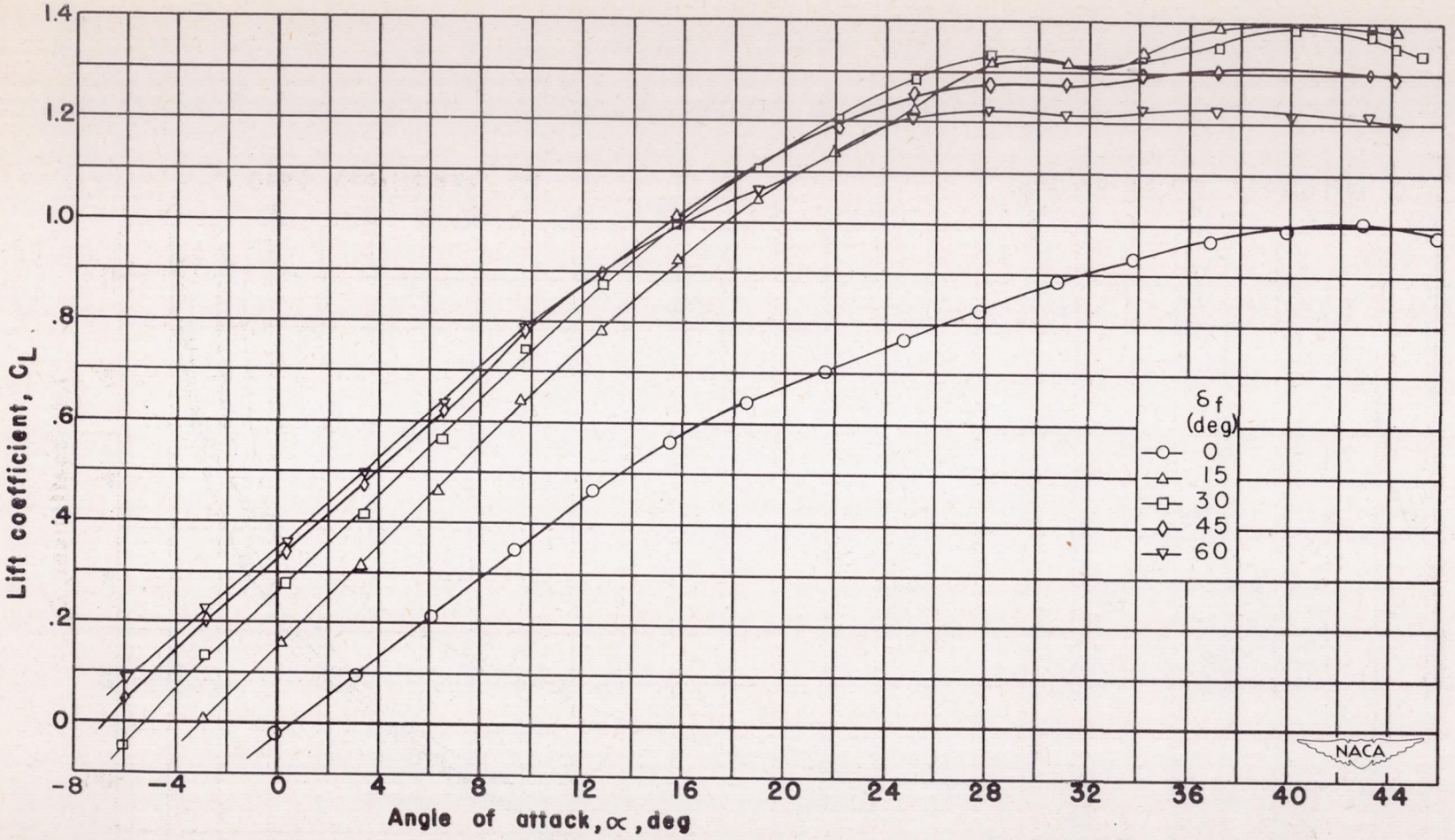
(a) C_L against α.

Figure 15.- Aerodynamic characteristics of 60° sweptback wing with six-step flap. q = 36.5 pounds per square foot.



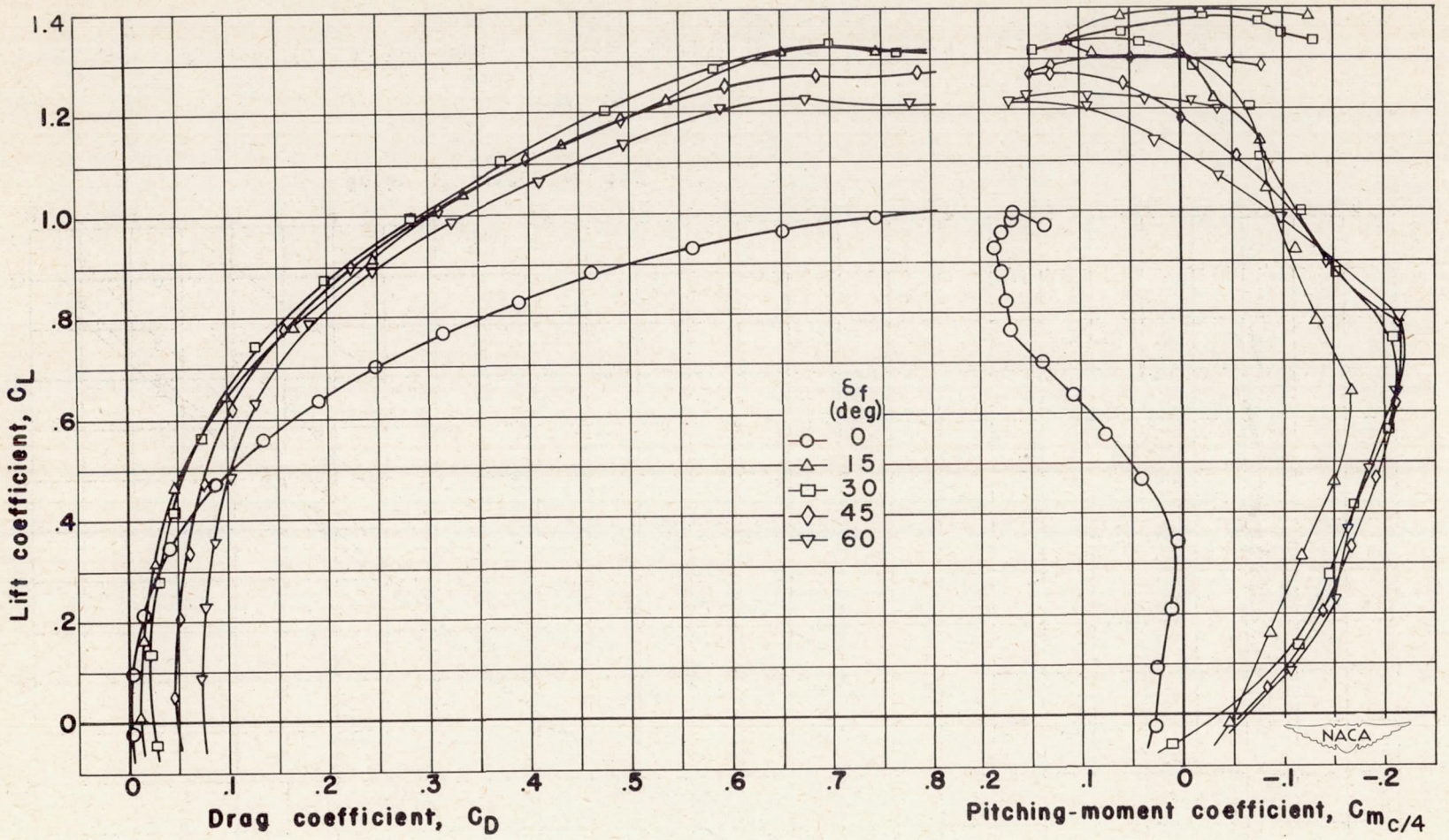
(b) C_L against C_D and $C_{m_{c/4}}$.

Figure 15.- Concluded.



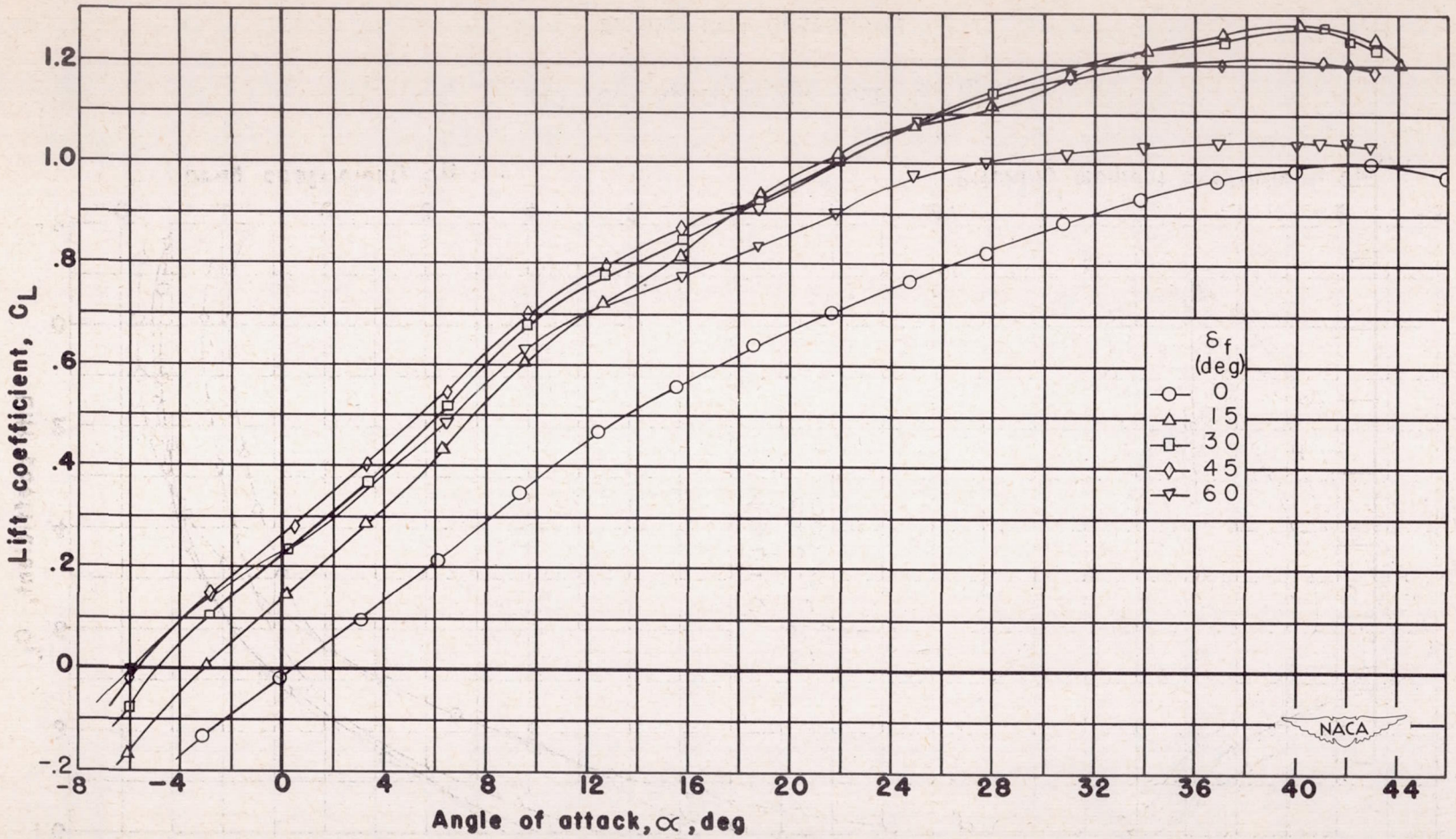
(a) C_L against α.

Figure 16.- Aerodynamic characteristics of 60° sweptback wing with slotted flap. q = 25.6 pounds per square foot.



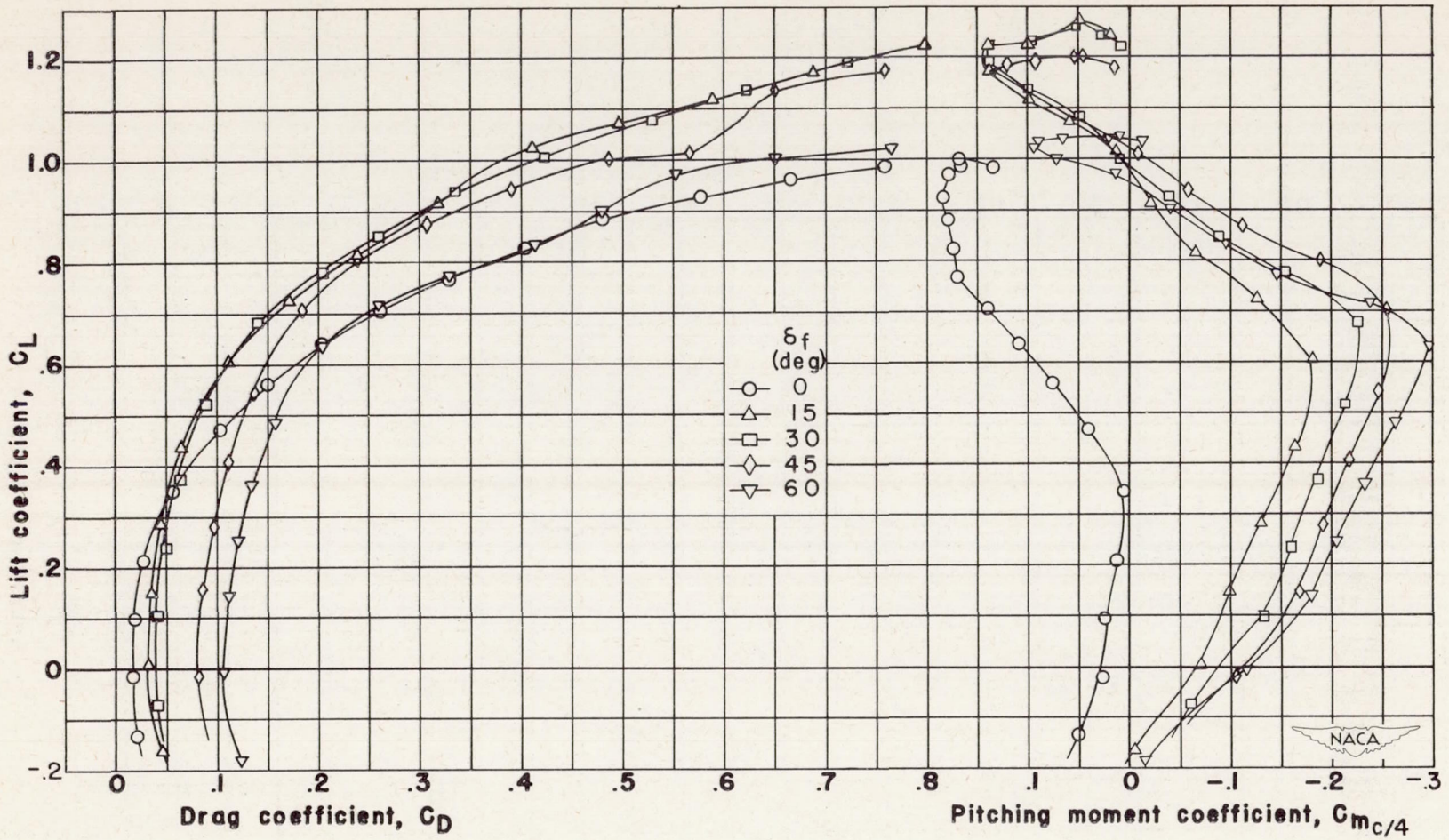
(b) C_L against C_D and $C_{m_{c/4}}$.

Figure 16.- Concluded.



(a) C_L against α.

Figure 17.- Aerodynamic characteristics of 60° sweptback wing with rotated slotted flap. q = 25.6 pounds per square foot.



(b) C_L against C_D and $C_{m_{c/4}}$.

Figure 17.- Concluded.

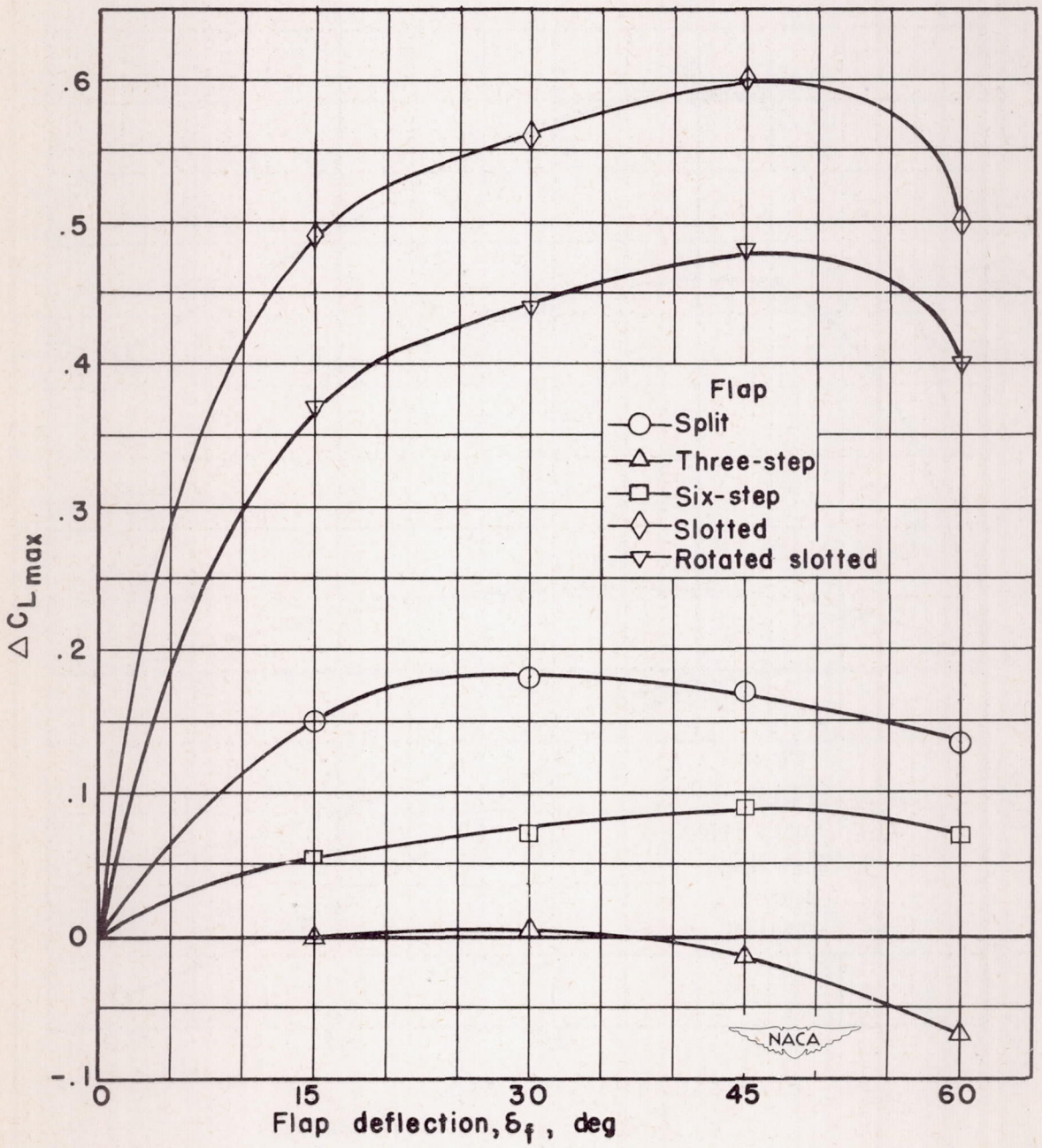


Figure 18.- Variation of $\Delta C_{L_{max}}$ with flap deflection on 45° sweptback wing.

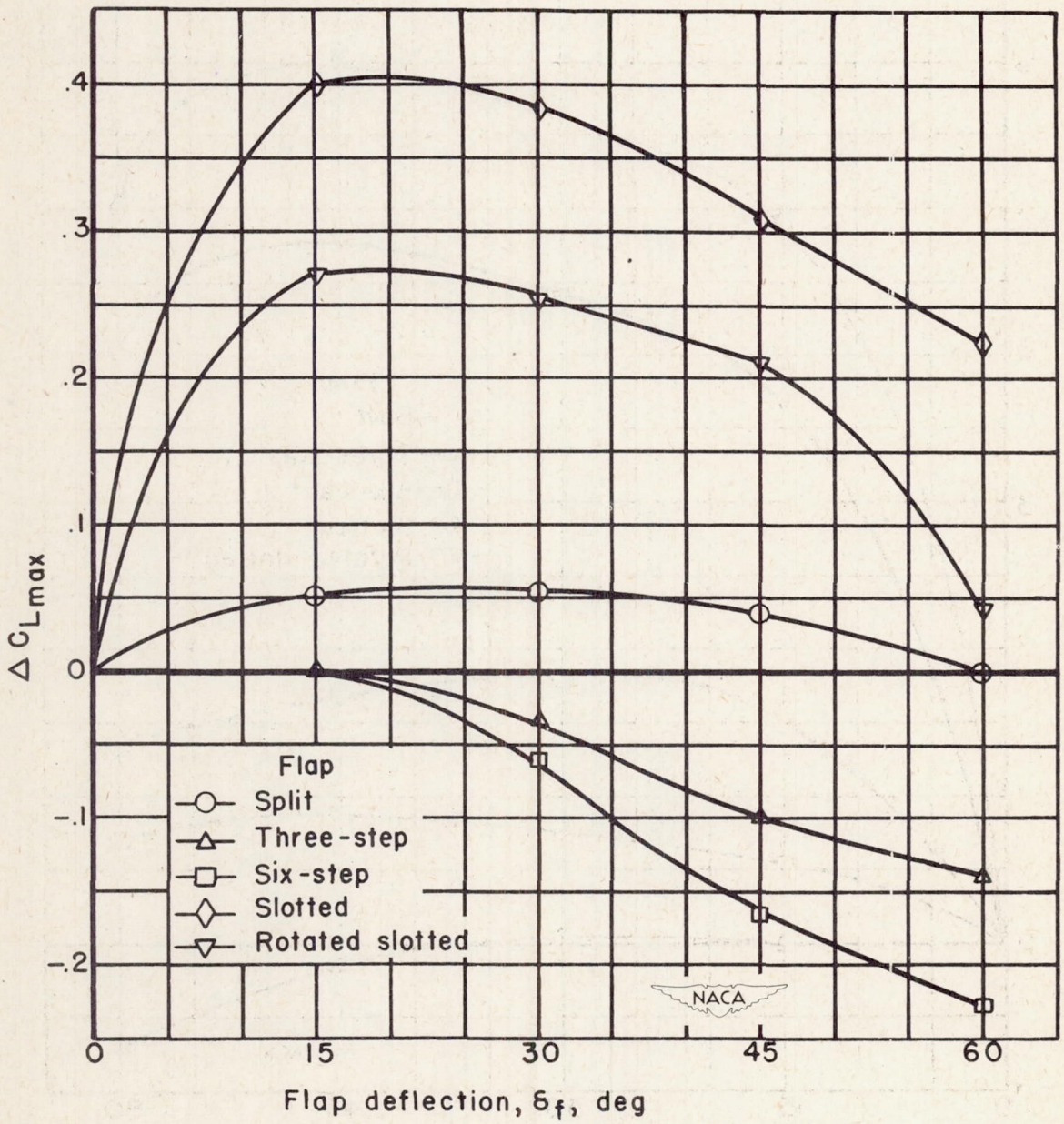


Figure 19.- Variation of $\Delta C_{L_{max}}$ with flap deflection on 60° sweptback wing.

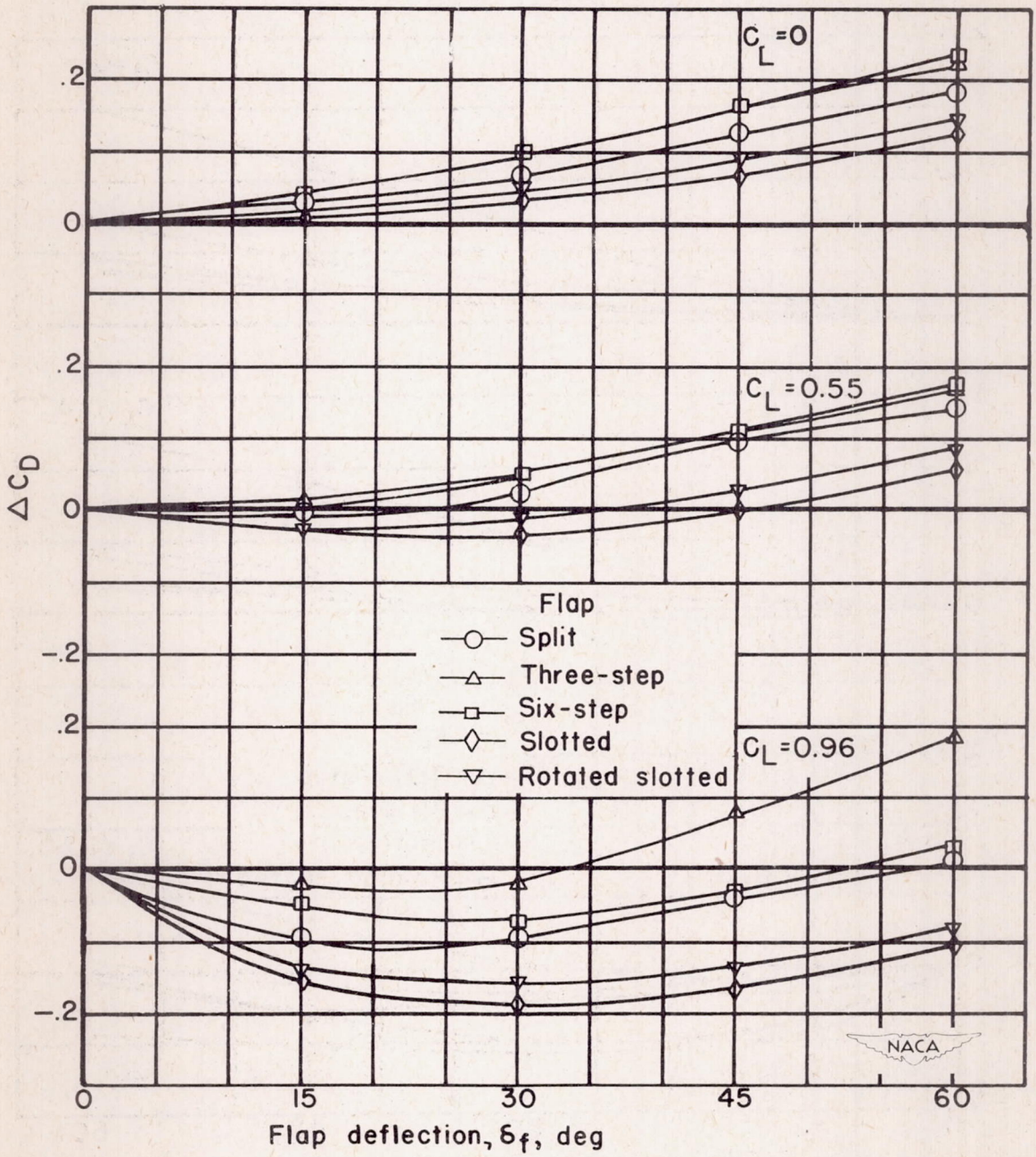


Figure 20.- Variation of ΔC_D with flap deflection on 45° sweptback wing.

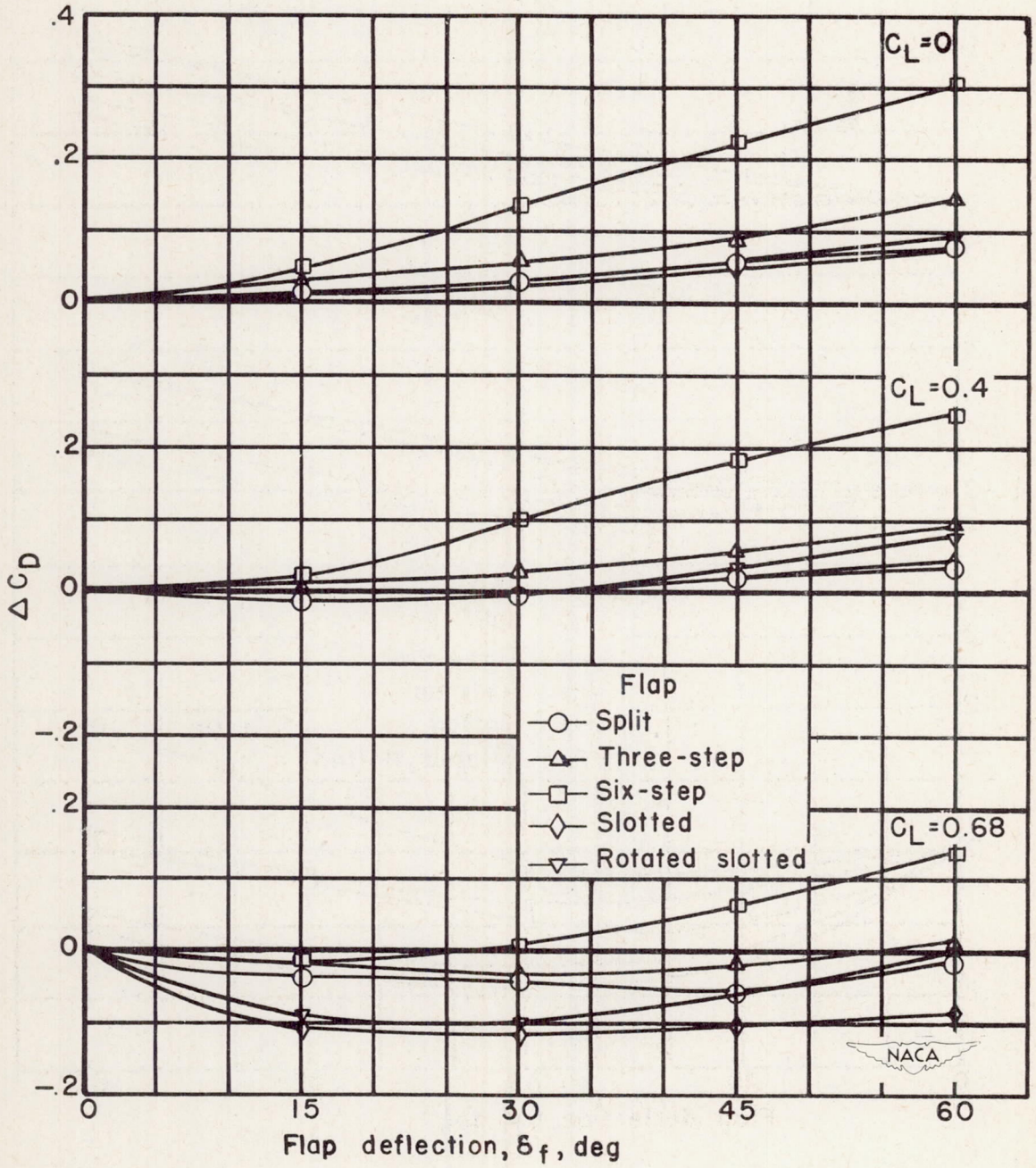
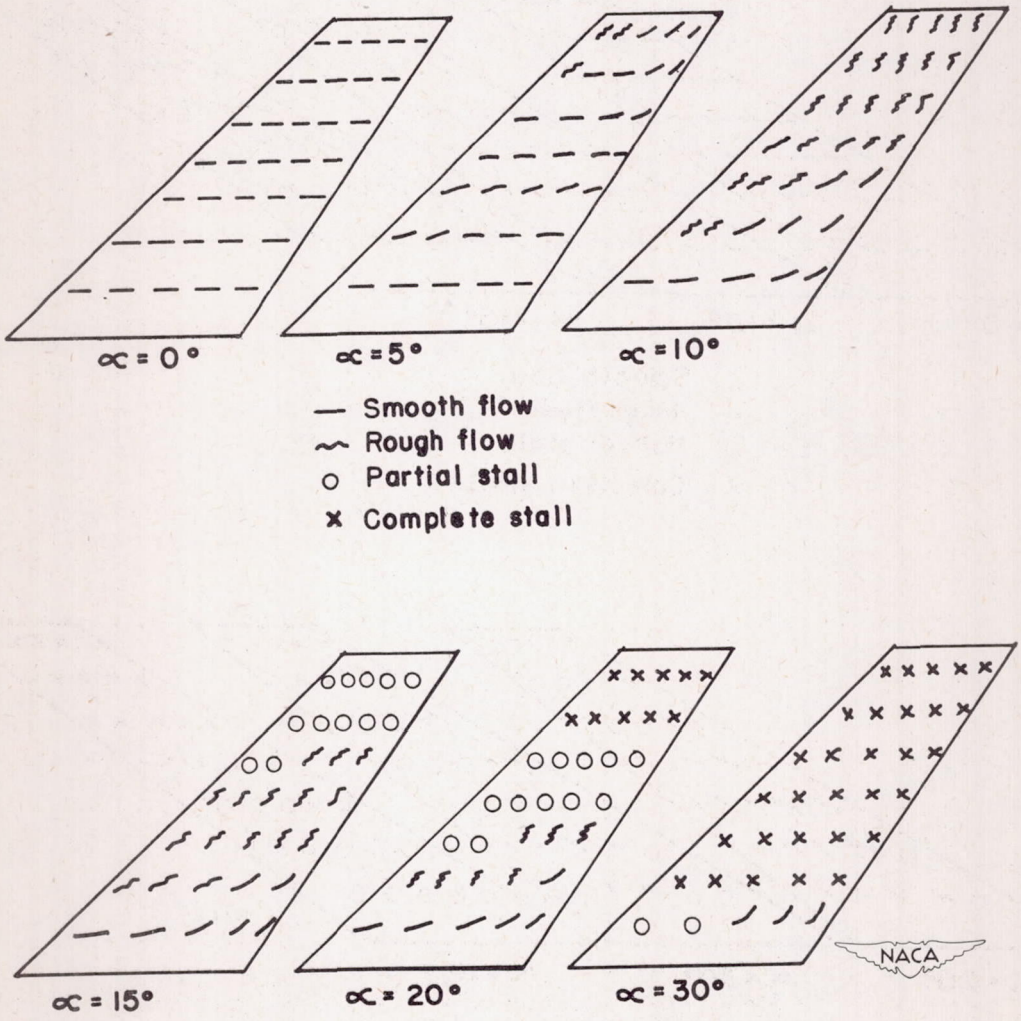
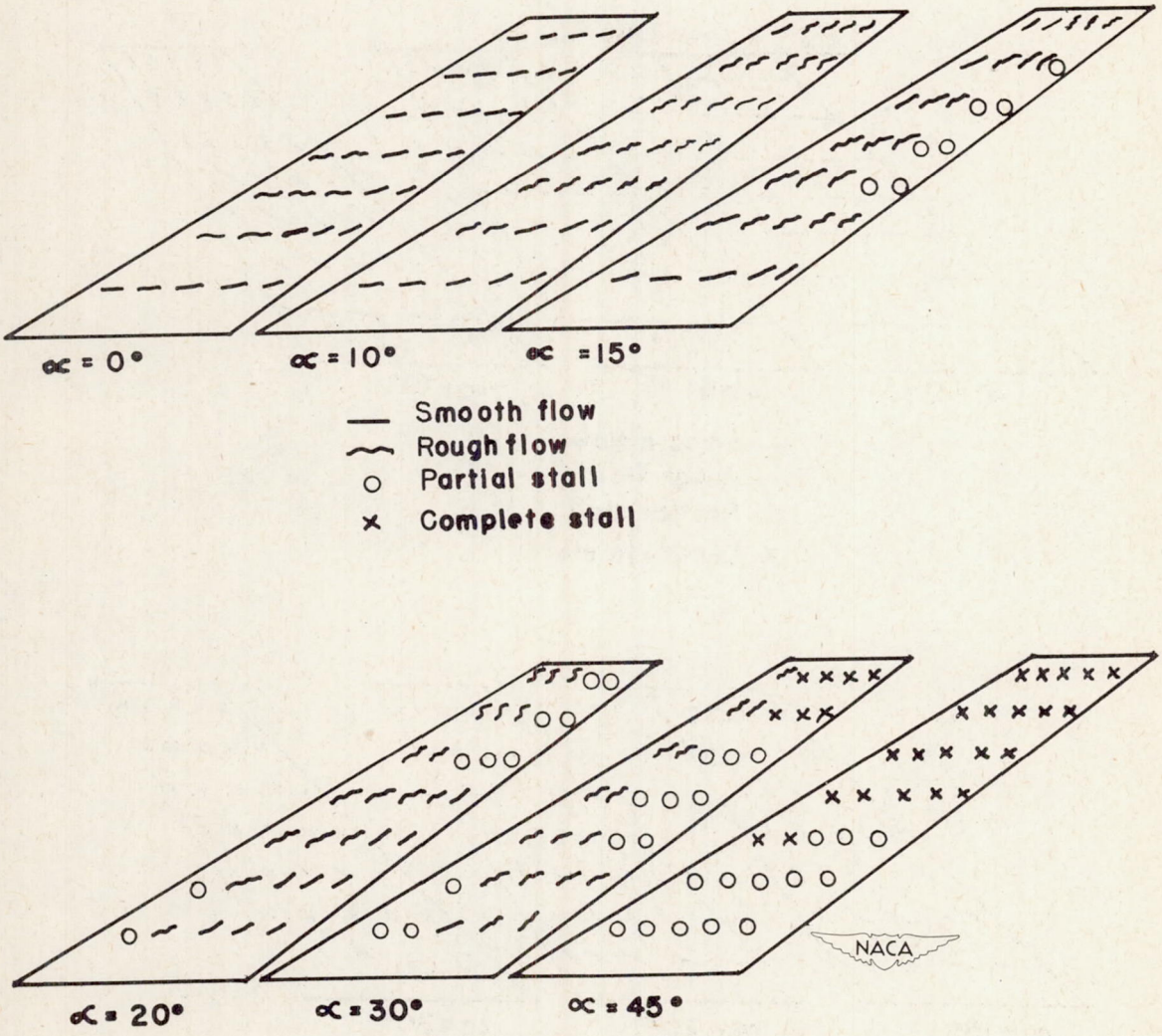


Figure 21.- Variation of ΔC_D with flap deflection on 60° sweptback wing.



(a) 45° wing.

Figure 22.- Tuft studies.



(b) 60° wing.

Figure 22.- Concluded.

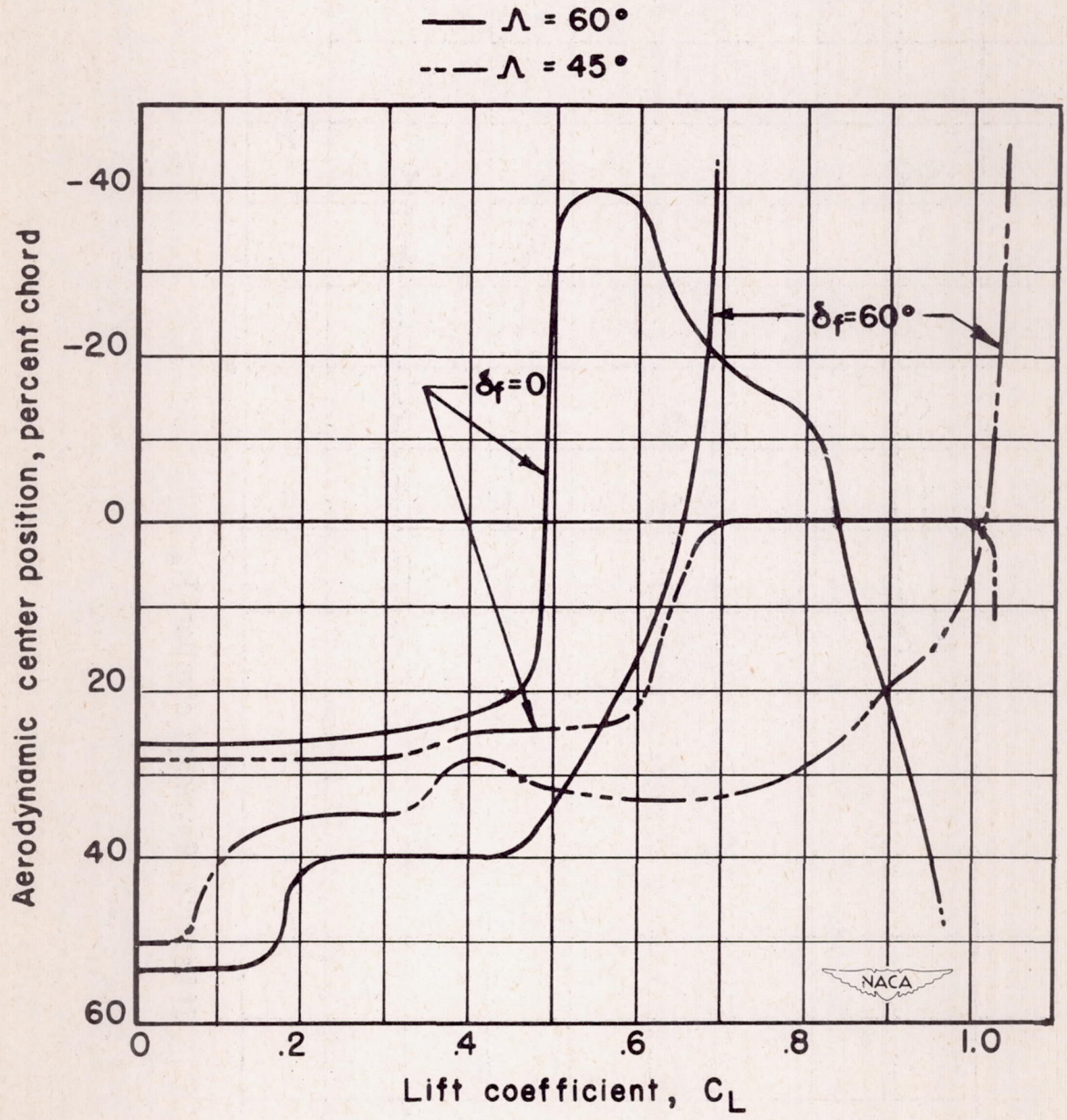


Figure 23.- Variation of aerodynamic-center position with lift coefficient with and without split flap.

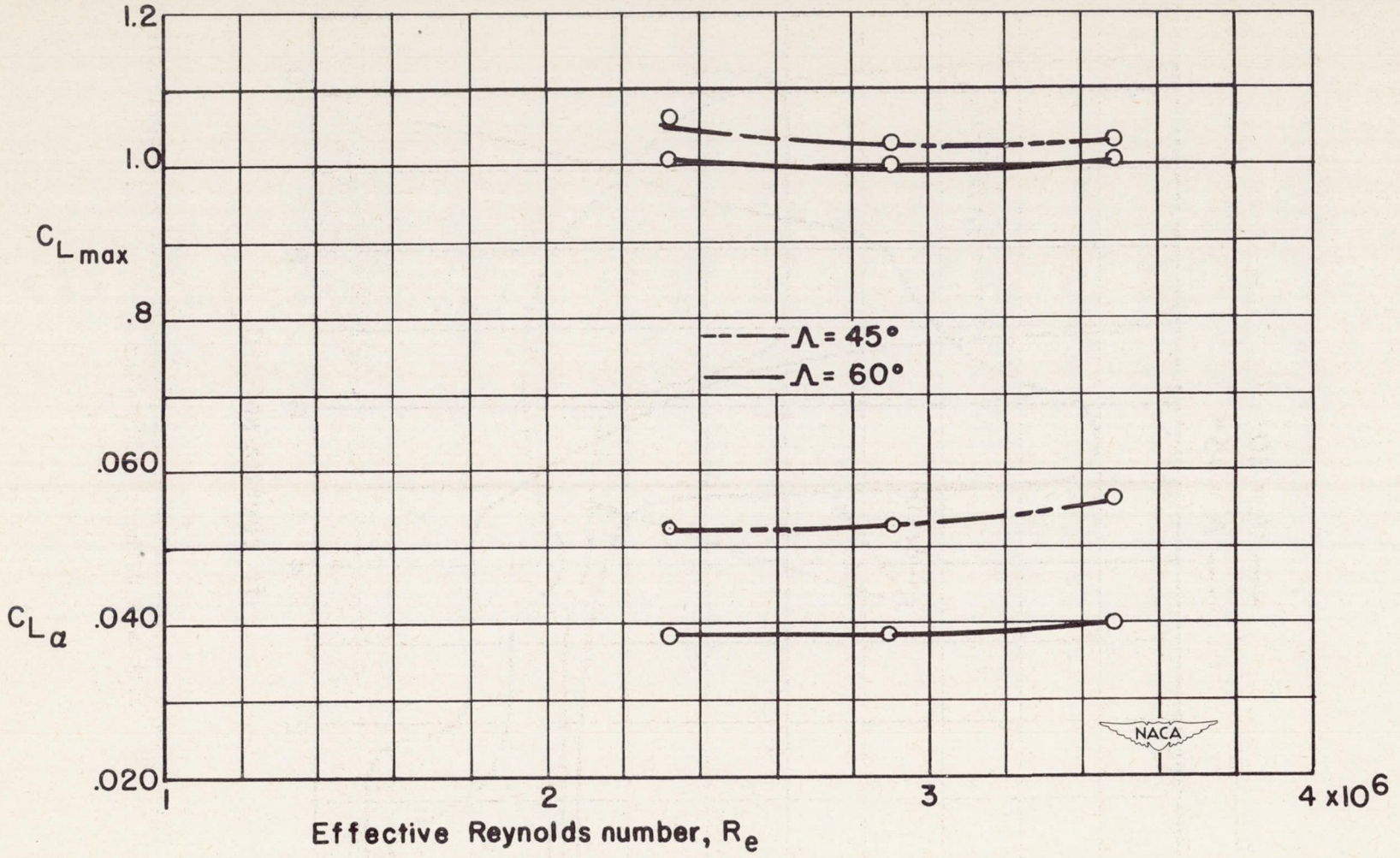


Figure 24.- Effect of Reynolds number on lift-curve slope and maximum lift coefficient.

NACA-Langley - 10-15-51 - 1000

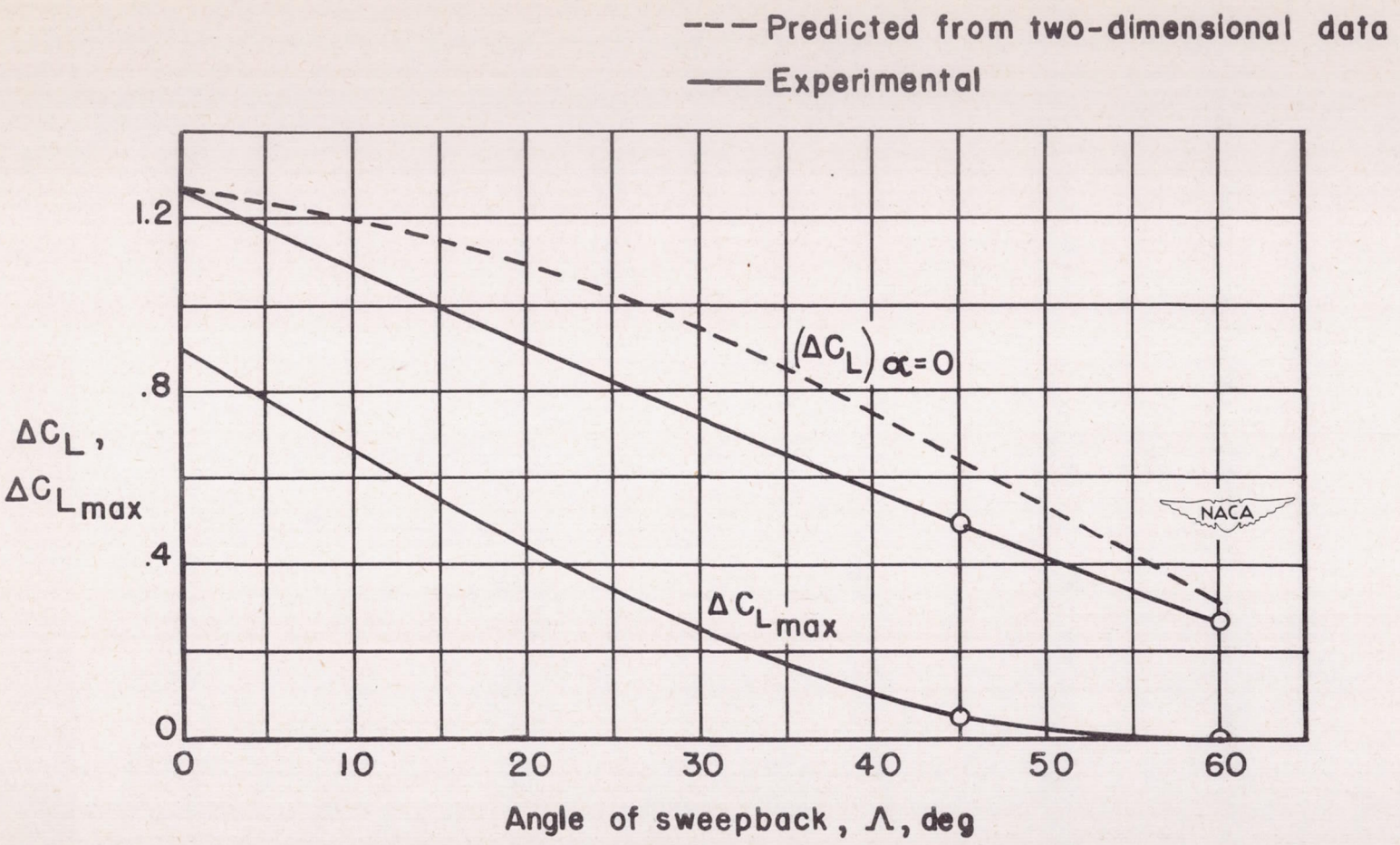


Figure 25.- Predicted and measured values of ΔC_L due to 60° deflection of full-span split flap.